metals

MDPI

Review

Deep Rolling Techniques: A Comprehensive Review of Process Parameters and Impacts on the Material Properties of Commercial Steels

Dilifa Jossley Noronha [1], Sathyashankara Sharma [1], Raghavendra Prabhu Parkala [2,*], Gowri Shankar [1,*], Nitesh Kumar [1] and Srinivas Doddapaneni [1]

[1] Department of Mechanical and Industrial Engineering, Manipal Institute of Technology, Manipal Academy of Higher Education, Manipal 576104, India; dj.noronha@manipal.edu (D.J.N.); ss.sharma@manipal.edu (S.S.); nitesh.naik@manipal.edu (N.K.); doddapaneni.srinivas1@learner.manipal.edu (S.D.)

[2] Department of Mechatronics Engineering, Manipal Institute of Technology, Manipal Academy of Higher Education, Manipal 576104, India

* Correspondence: raghu.prabhu@manipal.edu (R.P.P.); gowri.shankarmc@manipal.edu (G.S.)

Abstract: The proposed review demonstrates the effect of the surface modification process, specifically, deep rolling, on the material surface/near-surface properties of commercial steels. The present research examines the various process parameters involved in deep rolling and their effects on the material properties of AISI 1040 steel. Key parameters such as the rolling force, feed rate, number of passes, and roller geometry are analyzed in detail, considering their influence on residual stress distribution, surface hardness, and microstructural alterations. Additionally, the impact of deep rolling on the fatigue life, wear resistance, and corrosion behavior of AISI 1040 steel is discussed. Engineering components manufactured by AISI 1040 steel can perform better and last longer when deep rolling treatments are optimized with an understanding of how process variables and material responses interact. This review provides critical insights for researchers and practitioners interested in harnessing deep rolling techniques to enhance the mechanical strength and durability of steel components across diverse industrial settings. In summary, the valuable insights provided by this review pave the way for continued advancements in deep rolling techniques, ultimately contributing to the development of more durable, reliable, and high-performance steel components in diverse industrial applications. The establishment of generalized standardizations for the deep rolling process proves unfeasible because of the multitude of controlling parameters and their intricate interactions. Thus, specific optimization studies tailored to the material of interest are imperative for process standardization. The published literature on the characterization of surface and subsurface properties of deep-rolled AISI 1040 steel, as well as process parameter optimization, remains limited. Additionally, numerical, analytical, and statistical studies and the role of ANN are limited compared with experimental work on the deep rolling process.

Keywords: deep rolling; AISI 1040 steel; heat treatment; surface treatment; microstructure

Citation: Noronha, D.J.; Sharma, S.; Prabhu Parkala, R.; Shankar, G.; Kumar, N.; Doddapaneni, S. Deep Rolling Techniques: A Comprehensive Review of Process Parameters and Impacts on the Material Properties of Commercial Steels. *Metals* **2024**, *14*, 667. https://doi.org/10.3390/met14060667

Academic Editor: Lipo Yang

Received: 26 March 2024
Revised: 6 May 2024
Accepted: 10 May 2024
Published: 4 June 2024

1. Introduction

The influence of surface imperfections and surface/near-surface properties are crucial in the strength degradation and failure of engineering components or materials, especially at elevated temperatures. Surface/subsurface modifications can enhance the cyclic performance of components or materials primarily by increasing the surface yield strength, which attenuates fatigue crack nucleation and propagation [1]. To achieve these goals, surface/subsurface properties like surface finish, topography, hardness, and microstructure are altered and compressive residual stresses (CRSs) and work/strain hardening

are induced through surface treatments based on surface heat treating (e.g., carburizing, carbonitriding, laser/induction hardening), surface plastic deformation (e.g., peening, burnishing, deep rolling), or surface alloy modification (e.g., surface mechanical attrition, ion implantation, laser cladding, chemical or physical vapor deposition). However, to comprehend the maximum enhancement in fatigue performance, the processing parameters of the assumed surface alteration methods must be cautiously controlled in correspondence with the material of interest to nullify any undesirable effects (e.g., microcracks, unfavorable microstructure, non-homogeneity in induced CRS/cold work, etc.) during manufacture [1–3].

1.1. The Need for a Comprehensive Review of the Deep Rolling Technique

Fatigue of engineering structures/components, especially those experiencing frequent cyclic loads, is a common mode of failure that accounts for about 80–90% of all failures [2]. Practically, most of the failures that arise in industries initiate at the surface because of surface imperfections [3]. The industrial design requirements of engineering domains like aerospace (engine parts, turbine blades, structural components), automobile (shafts, bearings, gears, cams, valves, springs), power generation (turbine parts, pressure vessels, impellers, reactors), die and tool making (molds, forging and blanking tools, punches), biomedical (implants), etc., demand significantly improved fatigue performance without compromising with the design or load carrying capacity. The materials frequently used in these industries exhibit limited endurance with faster degradation of strength at higher cyclic amplitudes and elevated temperatures. Mechanical surface treatment/s (MST/s) is known to be the most viable option to enhance the fatigue performance of materials through altered surface/near surface properties with cost-effective and reduced process time benefits [4–6]. There have been consistent efforts by the research community in developing MSTs, optimizing the process parameters, and studying their effect on materials/components with an objective to achieve improved in-service performance [7–11]. However, it should be noted that the improvement in fatigue performance and surface properties are largely governed by the type and state of the material, the type of MST, and the process parameters.

Specifically, deep rolling is identified as the most viable MST owing to simple operation and tools, lower cost, and the highest level of beneficial surface properties when compared with contemporary techniques [12–14]. It is the most effective commercially available method used to enhance the fatigue performance of metallic materials owing to remarkable improvement in surface finishes, significant compressive depth, directional stresses, and work-hardened microstructures. However, standardizing the process is quite a challenging aspect considering the highest degree of influence of processing parameters on the material or component performance. Moreover, the type and initial condition of the material are crucial in achieving desirable properties through deep rolling. This indicates that each study is unique and necessitates the requirement of material-specific investigation with optimized parameters [11–14].

1.2. Mechanical Surface Treatments

Surface plastic deformation techniques, or mechanical surface enhancement techniques (MSETs), are recognized to be fast, clean, easy, and economical along with comparable surface properties among the available options [15]. MST/s involve a physical interaction between a tool and workpiece, which induces localized elastic–plastic deformations in the surface/near surface regions. This renders characteristic alterations in surface properties, which imparts strength and fatigue resistance to subsurface regions. However, the beneficial effects of MST/s prevail only if the modified surface properties are stable under cyclic loads and at elevated temperatures. A general classification of MST/s is presented in Figure 1, which mainly depends on movement between the workpiece and tool. Relative movement between the workpiece and tool comprises the burnishing and rolling

process, whereas no relative movement between the workpiece and tool comprises the different peening process, as shown in Figure 1 [15,16].

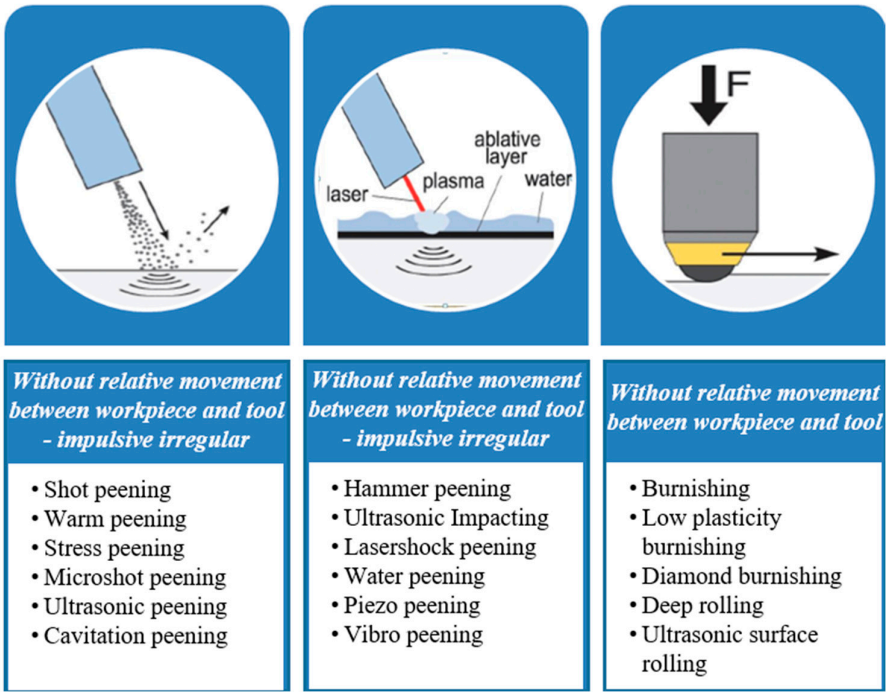

Figure 1. Classification of mechanical surface treatment techniques adopted with ref. [15] Wiley, 2005 and reprinted with permission from ref. [16] PLOS ONE, Creative Commons Attribution License, 2015.

1.3. Deep Rolling

Deep rolling (DR), or alternatively, deep cold rolling (DCR), is a mechanical surface treatment process adopted to convey a mirror finish to the surface and to induce a tailored microstructure, beneficial residual stresses, and cold work on the metal surface and near-surface regions with the help of a ball or roller end tool. The magnitude and stability of the induced surface/subsurface modifications through DR play a crucial role in improving the fatigue strength of a metal. It is an effective alternative to enhance the durability and surface hardness of a metal along with reducing the notch effect caused by surface microcracks. Moreover, deep rolling eliminates the need for costly and time-consuming secondary finishing processes such as polishing, grinding, plating, and surface heat treatments. It is a cost-effective technique when compared with other commercially available surface treatment techniques because of simpler tooling and processing on standard machines [17–20]. However, the use of this technique is limited to components with certain geometries or shapes owing to its working principle, and it is not suitable for components having significant variation in geometrical profiles, especially with thin walls and intricate areas with low tool accessibility. The working principle of the DR process is illustrated in Figure 2 [18,19].

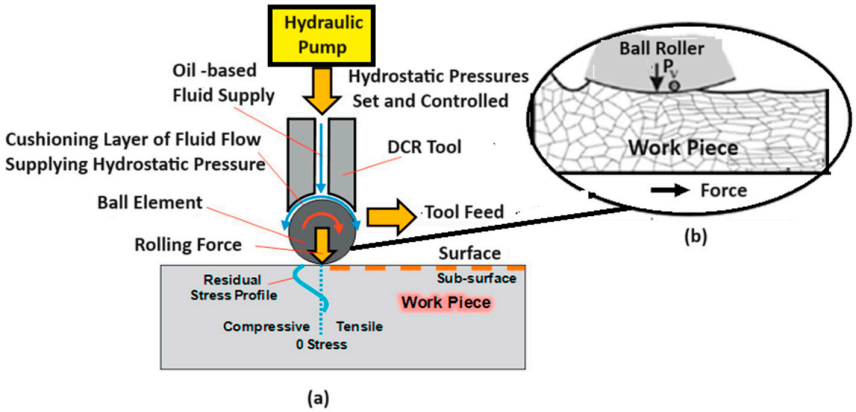

Figure 2. (**a**) Working principles of the deep rolling process reprinted with permission from ref. [21] ELSEVIER 2014 (**b**) Details of the tool and workpiece interaction adopted with ref. [22] SPRINGER 2016.

The specimen's surface is rolled over by a ball or roller. The deep grooves or sharp indentations on the surface are reduced by the ball's rubbing action, improving the surface finish. A plastic zone and a longitudinal groove are formed when the ball makes contact with the workpiece surface. The surface and near-surface regions up to a defined depth are plastically deformed, which encloses an elastically deformed core. Upon the separation of the ball, the recovery of the elastic zone creates large residual compressive stress on the surface. Significant compressive depth and cold work in about 1 mm (material-dependent) and directional strength enhancement (rolling direction-dependent) can be achieved [14,15]. In general, the operation of deep rolling can be realized through two motions as follows: (a) immersing or pressing the roller or ball (which is free to revolve about its own axis) against the workpiece with a pre-determined force and (b) rotating workpiece on the lengthwise axis (for cylindrical parts) or in-plane translations (for flat parts). The numerous controlling parameters illustrated in Figure 3 show the deep rolling process and, consequently, the near-surface properties [23]. Therefore, identifying the optimum combination of these control parameters is crucial for achieving desirable surface property enhancement.

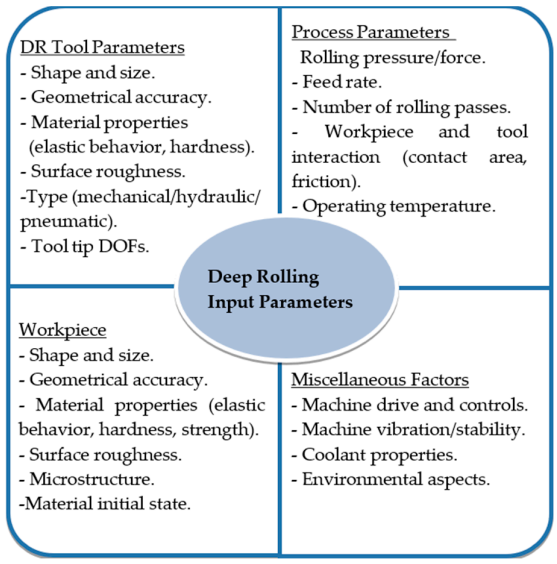

Figure 3. Classification of deep rolling controlling parameters adopted with ref. [23] DAVID PUBLISHING 2015.

1.4. Applications of Deep Rolling

1.4.1. Structural and General Applications

DR is most often used in industrial applications for those workpieces requiring enhanced properties paired with uncomplicated procedures at affordable costs. Specific applications involve (Figure 4) welded joints of structures, tubes, and pressure vessels, undercuts or stress-raising zones of parts, threaded parts, tension bolts, high-strength fasteners, torsion bars, gear tooth, cylinder bores, roller and thrust bearing race, heat exchanger tubes, and blanking punch fillets [24].

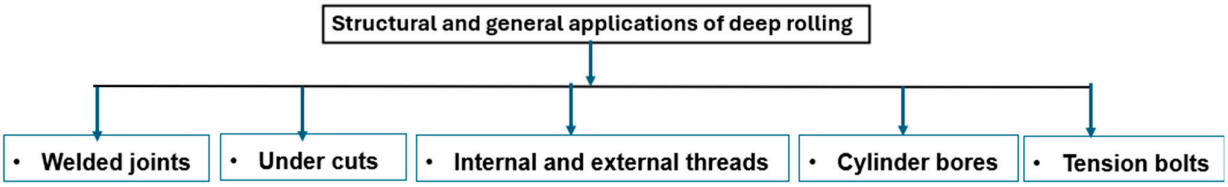

Figure 4. Structural and general applications of deep rolling.

1.4.2. Applications in the Automobile and Marine Industries

Strongly loaded axis-symmetrical elements like axles, shafts, crankshafts, steering knuckles, gears, valves, and similar propulsion and transmission system components are often deep rolled. In particular, weight saving is a prominent requirement for automobile components like steering wheels or propulsion systems, and hence, DR is efficiently used in these applications [12]. Figure 4 demonstrates the DR operation on common automobile components, and Figure 5 illustrates diesel marine engine crankshaft bearing surface deep rolling [25].

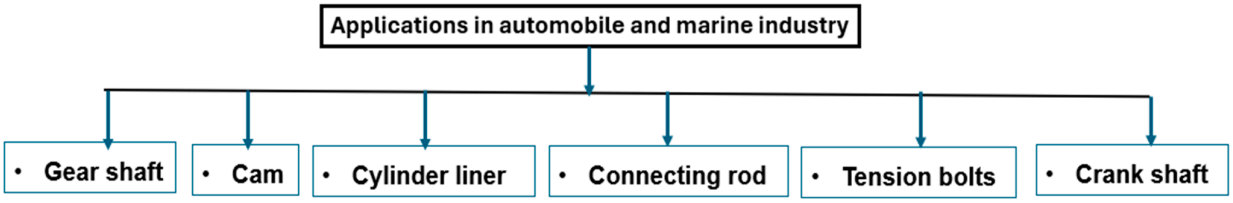

Figure 5. Deep rolling applications in the automobile and marine industries.

1.4.3. Applications in the Aerospace Industry

In aerospace applications, the major objective of designers is to minimize weight without compromising strength. DR, which provides notable surface/subsurface properties, is known to be the potential solution to achieve these objectives [12]. Typical examples shown in Figure 6 include heavily loaded structural parts like bolts and struts, propulsion parts like turbine discs, compressor rotor blades, transmission parts like landing gears, military aircraft wheel rims, etc. [8,24].

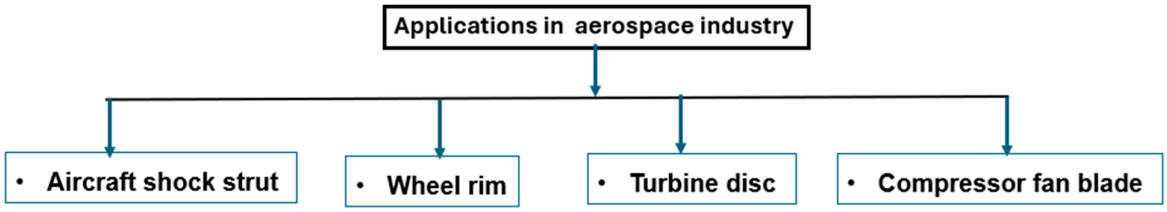

Figure 6. Deep rolling applications in the aerospace industry.

1.4.4. Applications in the Medical Industry

DR in the biomedical industry is mostly used for implant strengthening, which demands absolute surface optimization paired with longer fatigue lives with high loads. Typical examples include hip implants (Ti rods in total hip arthroplasty [26], components of Morse taper junctions in modular hip arthroplasty [27]) and spinal cord implants. In addition, elements of surgical tools that are cyclically treated under acidic and corrosive conditions may be reinforced by deep rolling to enhance stress corrosion resistance [12].

1.5. AISI 1040 Steel Material

AISI 1040 steel is an unalloyed medium/plane carbon steel with decent hardenability and mechanical properties. It is primarily utilized in as-bought untreated conditions for general-purpose structural applications, mostly for those that require higher strength steel when compared with mild steel while being cheaper than alloy steel. It exhibits good strength and toughness with a moderate surface hardness. Most heat treatments can be applied to AISI 1040 steel to adjust its physical and mechanical properties according to the user's requirements. In heat-treated form, it possesses homogeneous metallurgical structures, giving consistent machining properties and can be flame/induction-hardened to produce a good surface finish with moderate wear resistance (limited to sections of less than 63 mm). The material offers satisfactory corrosion resistance while exhibiting significant yielding before failure, which warrants safety measures over catastrophic failure. However, the material is not suitable for high shock loads as it shears under extreme conditions. Table 1 indicates equivalent/comparable steel grades in various material standards, and the chemical compositions and properties are listed in Tables 2 and 3 [28,29].

Table 1. Equivalent/comparable steel grades in various material standards.

AISI/SAE (ASTM A29)	IS (5517)	BS 970 (1955 EN)	BS 970 (1983/1991)	DIN (10083-1)	Werk Stoff	JIS (G4051)
1040	40C8	EN 8	080M40	C40	1.1186	S40C

Table 2. Chemical composition of AISI 1040 steel (in weight %).

Elements	C	Mn	Si	S	P	Cu	Fe
Range	0.35–0.45	0.6–1.0	0.03–0.35	0.06 (max)	0.06 (max)	0.06 (max)	balance
Standard	0.4	0.11	0.03	0.03	0.01	0.03	balance

Table 3. Properties of AISI 1040 steel (standard composition, cold-rolled).

Properties	Parameters	Metric Units
Physical Properties	Density	7845 kg/m^3
	Melting point	1521 °C
Mechanical Properties	Tensile strength	620 MPa
	Yield strength	415 MPa
	Elongation at fracture	25%
	Reduction of area	50%
	Elastic modulus	200 GPa
	Bulk modulus	140 GPa
	Shear modulus	80 GPa
	Poison's ratio	0.29
	Hardness (BHN)	201
	Hardness (HRB)	93
	Hardness (HRC)	13
	Hardness (HV)	211
	Izod Impact (as-rolled)	49 J
Thermal Properties	Coefficient of thermal expansion	11.3 µm/°C
	Thermal conductivity	50.7 W/mK

Applications of AISI 1040 Steel

AISI 1040 steel is used for applications that require better properties than mild steel at a cost much less than alloy steels. The material finds wide applications in structural and industrial sectors. The structural applications comprise steel cables, rods, tie wires, foundation bolts and studs, washers, and plates. In industrial applications, it is often considered for fabricating machines and their parts, carriage bolts, springs, and cylindrical parts such as valves, pistons of hydraulic or pneumatic cylinders, pump shafts, bearing bores, cold head parts, couplings, forgings, pressure vessels, oil rig parts, and mining tools. In the automobile industry, the material is used for general-purpose axles and shafts, crankshafts, keys, stressed pins, gears, tension bolts, cylinder head studs and springs, rails, railway wheels, and rail axles. However, fatigue failure is the decisive factor in the service life of these components, which makes the use of fatigue strength enhancement techniques like deep rolling crucial for this material.

The present research examines the various process parameters involved in deep rolling and their effects on the material properties of AISI 1040 steel. Key parameters such as rolling force, feed rate, number of passes, and roller geometry are analyzed in detail, considering their influence on the residual stress distribution and surface hardness. Additionally, the impact of deep rolling on the fatigue life, wear resistance, and corrosion behavior of AISI 1040 steel is discussed. The Artificial Neural Network (ANN) is a well-known method used in many industrial fields. It is inspired by the neural structure of the human brain and processes information through interactions among many neurons. To the best of the authors' knowledge, however, there has not been any attempt to specifically use an ANN to anticipate deep rolling effects in publicly accessible studies and publications. In conclusion, the establishment of generalized standardizations for the deep rolling process proves unfeasible because of the multitude of controlling parameters and their intricate interactions. Thus, specific optimization studies tailored to the material of interest are imperative for process standardization.

2. Literature Review

In this section, a detailed review of the literature on the DR process and tooling is presented. An effort was made to comprehend the DR process, identify the crucial process parameters, optimization techniques, methodologies, effects of DR on material/component performance, efficiency of DR when compared with other MSTs and/or relevant surface treatment processes, etc. Furthermore, the literature on the design and development of DR tools was reviewed to recognize various types of designs and mechanisms with specific emphasis on identifying the tool design requirements.

2.1. The Deep Rolling Process

The literature available in the published domain highlights consistent efforts by the research community in innovating, developing, and standardizing the DR process. Though some of the literature practices the use of term burnishing, specifically low plasticity burnishing (LPB) and deep rolling alternatively, owing to similar principles, there are significant and reliable works that clearly differentiate the two based on their objective. The primary objective of DR is to enhance fatigue life through significant cold work on the surface/subsurface regions, which induces strain hardening and a higher depth of residual stress profiles, while the burnishing process is primarily performed to ensure a smoother surface finish and has little effect on fatigue life.

K. H. Kloos et al. [30] suggested that DR could be a potential alternative surface treatment technique for enhancing material strength. Their study performed on 37CrS4 steel deep-rolled smooth and notched specimens indicated that DR fully nullifies the notch effect when performed with optimized parameters. It was demonstrated that DR substantially enhanced the material performance more than that attained through surface hardness enhancement techniques like heat treatment, especially in the case of notched

specimens. This was attributed to the dominant effect of DR-induced CRS on retarding crack propagation in bending fatigue, which was absent for the latter. Moreover, the work revealed that the rolling load could be the key parameter for defining the DR process and, its optimization is crucial for realizing pertinent benefits. Hertzian contact theory and/or von Mises distortion energy theory, which yields equivalent stress, was reported to be the appropriate method for describing DR conditions.

D. Meyer and J. Kammler [31] acknowledged that mechanical energy-induced cold surface hardening techniques, specifically DR, could be a sustainable alternative for heat treatment-free surface modification. It was demonstrated that DR as a single process enabled a work-hardened martensitic surface coupled with excellent surface finish in metastable austenitic steels when compared with combined thermal treatment followed by finishing operation. This was reported to be beneficial in reducing the process time along with eliminating energy-consuming thermal treatment techniques resulting in faster and efficient production of hardened steels.

I. Altenberger [12] reported superior surface finishes and higher fatigue lives for several steels with DR over contemporary MSETs like shot peening (SP), ultrasonic shot peening (USP), and similar performance as that of laser shock peening (LSP). However, DR at an elevated temperature (at 350 °C) showed a more considerable improvement in performance than LSP. Moreover, the case depth was comparable to that attained by thermochemical treatments like nitriding. This shows DR is an extremely powerful tool for enhancing the fatigue performance of several types of steel (SAE 1045, AISI 4140, AISI 304, custom 450 stainless steel) through mechanical surface optimization. In addition, the author marked the significance of DR on harder titanium alloys or lighter magnesium alloys in enhancing the near-surface properties.

J. Scheil et al. [32] investigated the influence of hammer peening (HP) and DR process parameters on the surface hardness of cast irons (EN-GJL-250 and EN-JS2070), tool steel (1.2379), and cast steel (GP4M) through experiments. Moreover, statistical techniques were employed to establish an appropriate combination of process parameters for both HP and DR processes, while additional FE simulations were performed for the latter. The FE modeling was used to predict cold work through displacement and accumulated plastic strain. Their findings showed that a direct comparison of HP and DR process parameters is not conceivable. However, a higher degree of enhancement in material surface hardness was reported with DR.

A. Klumpp et al. [10] presented a review of several MSETs and discussed the effect on surface layer states of quenched and tempered AISI 4041 steels. From the discussions presented, DR appears to be the most viable option for ensuring the deeper penetration of CRS and cold work with a remarkable surface finish for the considered material. However, their investigation pointed out that the attained surface layer states were sensitive to variations in process parameters. This allowed for only a certain degree of freedom, and each MSET displayed specific individual limits with respect to achievable surface characteristics. The effectiveness of MSETs was reported to be governed by process principles (impulsive, static, etc.), process constraints (pressure, feed rate, speed, number of passes, etc.), the initial state of the workpiece (hardness, geometry, roughness, etc.). and the ambient conditions (temperature, etc.). They emphasized that the optimization of these characteristics and their interactions is decisive for utilizing the process benefits to the maximum extent.

Similar studies involving assessing various MSETs (DR, SP, LSP, etc.) and their effect on engineering materials (steels, Al alloys, Mg alloys, Ni alloy, Ti alloys) emphasize the requirement of process optimization to ensure the greatest effect on surface/subsurface characteristics [5–9,33]. It is important to note that each process has its own limitations. For instance, processes like LSP can provide superior surface properties in certain materials (e.g., Ni alloys, Ti alloys, or some specific steels) over DR because of material-specific behavior. However, DR, being the simplest of all, yields in par/superior results for most steels and Al alloys when performed with optimized conditions. Nevertheless, the exact

comparison of MSETs is vastly arbitrary in nature owing to significant divergence in the principles and varied responses of materials. These studies suggest application-specific adoption of appropriate MSET and recommend considering physical and mechanical characteristics (microstructure, surface topology, hardness, CRS, and cold work) over the use of empirical methods for process parameter optimization. This indicates that establishing universal guidelines for ensuring optimized outcomes is challenging and represents a higher degree of uncertainty involved in MST processes.

P. Juijerm et al. [34] and I. Altenberger et al. [35] extensively studied the effect of DR at varied temperatures on several materials (SAE 1045 and AISI 304 steels, AA 5083 and AA 6110 alloys, Ti-6Al-4V α-β Ti alloy). The work showcased enhanced physical and mechanical properties in all the considered materials when deep-rolled. However, the material responses were quite diverse compared with DR parameters, which was reflected in the characterized near-surface properties and cyclic performance. This demonstrates the requirement of material-specific studies to uncover the full potential of DR to achieve optimized material performance.

Altenberger and B. Scholtes [7] highlighted the effect of induced microstructure and CRS in the near-surface regions of SAE 1045 steel by DR and SP on mechanical properties and fatigue behavior. The results showed excellent improvement in the considered material behavior compared with non-treated samples, while DR was superior to SP. The authors recommended the use of physical and mechanical principles for process optimization over the empirical method and stressed the significance of XRD for material characterization, especially for CRS.

A. M. Abrao et al. [17,36] extensively studied the effect of DR process parameters on the surface integrity, hardness, microstructure, CRS states, and stability under cyclic loads for AISI 1060 steel material. Their study revealed that the initial state of the material, rolling pressure, and rolling passes had the most significant influence on the realized benefits of DR. It was noted that the lower the initial material hardness, the higher the sensitivity to DR and the better stability of the induced surface alterations under cyclic loading. With increasing pressure and number of passes, the ultimate strength increased, while the yield strength and surface roughness decreased. This was attributed to the higher cold work and distribution of dislocations. Brittle fracture was reported for deep-rolled hardened steel samples, which was obvious due to induced cold work. Unfortunately, the effects of process parameters on the surface/subsurface region microstructure and its influence on mechanical properties were not elaborated.

F. F. Do-Santos et al. [37] explored the effect of DR on the surface integrity of AISI 1020 steel. It was reported that DR significantly enhanced the surface properties in comparison with untreated samples within stated conditions. The improvement in surface finish was attributed to plastic deformation, which displaced the material from peaks toward valleys, thus promoting flatness. However, excessive pressures, which cause shear-induced surface instabilities and higher feed, thus reducing the treating points, showed adverse effects on surface finish. Moreover, it was suggested that the feed must be less than that used for previous machining for deforming roughness peaks. The microhardness on the surface was reported to be either maintained or reduced after DR, albeit an increase in subsurface microhardness was observed. It was believed that the excessive homogenization of pre-existing dislocations over the surface after DR led to the reported retention/decrement in surface microhardness. An increase in rolling pressures and feed supplemented the subsurface microhardness, which was attributed to strain hardening caused by dislocation pinning in the subsurface regions. The reduced microhardness and affected depth observed for increased roll passes were attributed to the homogenization of induced dislocations in subsequent layers beneath the surface. The microstructural analysis revealed an increase in deformation with rising pressure and rolling passes; however, a rise in speed and feed was reported to have a detrimental effect. The increased deformation was believed to be the effect of increased stresses at higher loads and the accumulation of deformation with increased passes. The reduction in deformation was

attributed to reduced contact time (in the case of increased speed) and reduced overlap (in the case of increased feed).

Furthermore, F. F. Do-Santos et al. [38], in another work, reported the impact of the carbon fraction on the surface properties of steels (AISI 1020, AISI 1065, AISI 1080) when deep-rolled. The DR control parameters (rolling pressure, speed, feed, and rolling passes) were correlated with the surface/subsurface properties, namely, roughness, hardness, and microstructure. It was observed that DR offered substantial enhancement in inspected material properties. The rolling pressure was observed to be the most critical parameter that governs the attained surface finish. However, an excessive increase deteriorated the surface condition. The work indicated that this could be countered by increasing the carbon content. The roll passes and speeds were reported to have negligible impact on the achieved surface finish within assumed conditions. Interestingly, it was observed that the rolling feed rate set close to the prior machining operation deteriorated the surface which was accompanied by an increase in carbon content. An increase in surface microhardness for AISI 1080 steel was observed in contrast to the retention/further reduction in AISI 1065 and AISI 1020 steels. This was attributed to the generation of additional dislocations associated with high carbon content in the former compared with the latter. Subsurface microhardness was reported to increase for all the steels in consideration. However, the affected depth was noted to be reduced with an increase in carbon content, which in turn increased mechanical strength and offered resistance for cold work during DR. The increase in rolling pressure and roll passes caused higher grain deformation in low-carbon content steels, while a larger speed and feed lessened it. Moreover, for AISI 1080 steel, only an increase in feed caused significant grain deformation, while all other parameters showed no/little effect. The elevation in the carbon content was believed to resist grain deformation, which justified the variation in the material response observed for DR.

The effect of DR with varied process parameters on AISI 304 steel, which is typically used in austenitic stainless steel in aerospace, chemical, surgical, and food industries, is well documented [39–41]. These studies reassure the use of DR for enhancing material surface properties and, thereby, cyclic performance. It was noted that DR evolved complex surface/subsurface microstructure, which displayed deformation bands, nanocrystalline regions, and martensitic twin lamellae induced by cold work with severe dislocation densities in the austenitic matrix. Deep Rolling at Elevated Temperature (DR-ET) was testified to yield higher fatigue life, albeit Deep Rolling at Cryogenic Temperature (DR-CT) did not improve the fatigue life compared with Deep Rolling at Room Temperature (DR-RT) despite a larger martensitic structure. The stated work clearly highlights the significance of the stability of DR-induced surface modifications to achieve optimum material performance, which is strongly dependent on cyclic stress amplitude, cycle count, and temperature. The work-hardened nanocrystalline surface layers were reported to be more stable than CRS within the reported conditions, and the relaxation mechanism under applied loads (thermal/mechanical) was thought to be governed by thermally activated gliding of dislocations.

J. M. Cubillos et al. [42] investigated the effect of DR and its parameters on the fatigue performance of AISI 304 and AISI 316 steels for comparison purposes with an aim to identify the potential of using the materials alternatively. It was observed that the improvement in surface finish and hardness in both materials was predominantly dependent on rolling pressure, while the effect of rolling speeds on the latter was insignificant. The improvement in fatigue life in both materials was obvious due to DR characteristics. However, apart from very high cycle fatigue, where AISI 304 showed superior performance, all other reported properties were comparable with each other, as expected because of the obvious similarities in materials. Metallurgical aspects like the formation of deformation twins and marginally higher martensitic phase were assumed to be the reason for differentiable fatigue behavior, albeit the same was not explored.

A. Tadi et al. [43] reported the effect of DR specifically focused on induced nano/ultrafine structures in the surface/subsurface regions of AISI 316L steel. In contrast to most

of the works reported in the literature, in the said work, a large number of rolling passes (specifically 15 and 26 passes) were applied. The outcome of these works supports DR as an excellent technique for inducing boundary layer grain refinement and a strain-hardened martensitic structure through multiple passes, which results in a significant increase in surface hardness with deeper penetration. However, the studies were limited to microstructure, hardness, and tribological property analyses, which could be due to the intended application.

P. R. Prabhu et al. [44,45] extensively investigated the effect of turn-assisted DR on the physical and mechanical properties of AISI 4140 steel material with the objective of optimizing the process. Several DR controlling parameters, namely, rolling ball material and size, rolling force, number of roll passes, initial surface roughness, coolant, feed rate, and speed, were considered, which are acknowledged to have a direct correlation with achieved material properties. Experimental, numerical, and statistical methods were employed to optimize the process parameters. A larger rolling force, a larger ball diameter, and an increased number of rolling passes along with low initial surface roughness were identified to be the preferred combination for realizing the greatest level of benefits. The nature of the DR effect predicted through numerical simulations was observed to be appropriate. However, significant divergence in the estimated magnitudes was reported in correlation with the measured parameters. These variations were attributed to limitations with 2D FE simulations. The reported practice of statistical method was observed to be a successful approach for dealing with the highest level of uncertainties involved with optimizing DR process parameters owing to their diversity and complex interactions. Unfortunately, the role of residual stress states in circumferential and longitudinal directions and altered microstructures in surface/subsurface regions in the realized benefits were not explored. Nevertheless, their findings divulged the potential of DR as a surface enhancement technique that demonstrates improved fatigue performance within assumed conditions.

Furthermore, in another work, P. R. Prabhu et al. [46] discussed the influence of DR on surface properties along with the corrosion behavior of AISI 4140 steel. Their findings showed, among the considered DR control parameters, that the rolling force and rolling ball size along with the number of roll passes had a significant influence on surface properties, primarily roughness and hardness. The corrosion rate was reported to be lower in the treated samples in comparison with the untreated samples, which was attributed to an altered grain structure, enhanced surface finish, and increased surface hardness coupled with induced CRS through DR. The rolling ball diameter and interaction effect of the initial surface roughness with rolling force were reported to have the highest level of impact on the observed corrosion behavior. In addition, the authors presented an empirical model for estimating the corrosion rate, which verified the measured values. The work revealed that DR could be an effective alternative for enhancing the corrosion resistance of steels within stated conditions.

N. Lyubenova et al. [47] analyzed the impact of process parameters (rolling pressures, number of passes and overlap percentage, pre-machining state, and measurement techniques) on the CRS state in deep-rolled AISI 4040 steel material. Their findings derived ambiguous conclusions indicating a high degree of interaction among the considered process parameters. However, in all the cases, DR had a significant influence on the generated CRS state when compared with untreated conditions. It was stated that despite the well-acknowledged advantages of the DR process, the control of CRS penetration depth and magnitude is still a challenge because of the complex interaction of several process variables.

A. M. Martins et al. [48,49] extensively investigated the effect of DR on the fatigue life of AISI 4140 steel material along with considering the influence of machining parameters. Although it was acknowledged that DR enhanced the fatigue life of turned samples in most instances, in specific cases, DR was not fully effective in eliminating the detrimental effects, particularly in the samples turned with higher feed rates. However, longer fatigue

lives observed in these samples were attributed to a greater influence of turning feed rather than the full benefit of DR. This indicates that machining parameters greatly influence the realized benefits from DR and, thus, material in-service performance. Therefore, DR process control parameters and their levels must be carefully decided based on previous machining constraints to achieve optimized performance. In addition, it was reported that apart from imparting enhanced fatigue performance, DR altered the location and form of fatigue fracture, which are believed to be additional benefits.

In contrast to numerous discussions available in the literature on correlating DR process control parameters with ensuing surface/subsurface properties, D. Meyer and J. Kammler [50] proposed an approach that relied on the internal material loads developed by applied external pressures for regulating desired material modifications. DR was performed on AISI 4140 steel cylindrical specimens with varying rolling pressures and ball diameters. However, a high feed was assumed to differentiate each rolling track and avoid overlapping. Equivalent stress according to Hertz was considered the internal variable parameter as a response to applied external variable process parameters. The study revealed that correlating the mechanism of DR, i.e., considering internal parameters, namely, equivalent stress or strain, for regulating desired surface modification (process signatures) could be the most viable option over the conventional approach. In addition, the authors suggested the use of numerical approaches could be beneficial in correlating the internal and external parameters and/or material modifications. However, their work did not highlight the role of other significant DR parameters like number of passes, feed, speed, material state, etc., on the internal parameter. In addition, the Hertz contact theory adopted for determining internal parameters does not fully rationalize the DR process mechanism.

J. Kammler et al. [51] showed that correlating internal loads with material modifications offers a better prediction of altered surface characteristics in multistage DR. Equivalent stress determined using Hertz theory was considered the internal parameter for correlation with material modifications, specifically CRS. The study performed on AISI 4140 steel flat specimens demonstrated that considering external process parameters specifically, rolling force may not fully justify the assumed surface/subsurface properties, while the correlation with internal loads could be an effective alternative. Unfortunately, the work relied on Hertz contact theory for predicting internal parameters, which may not be appropriate to realize the elastic–plastic state of stress developed in the DR process fully.

Apart from steels, the possibilities of using DR to enhance the properties of several other engineering materials that find profound applications in industries were explored in the past. For instance, light materials like Mg alloys [52–54] or Zr alloys [55]; softer materials like Al or Cu alloys [56–62]; hard and difficult-to-machine materials like cast irons [32,63], Ni alloys [64–66], or Ti alloys [67–69]; composite materials like Al-SiC [70,71] were demonstrated. All these studies reported excellent improvement in properties of interest in the assumed material when compared with untreated conditions. However, the degree of improvement observed varied with the considered DR parameters and material-specific behavior. A detailed review of the influence of DR and its parameters on the physical and mechanical properties of these materials is well-documented elsewhere [5,6,11,33,72] and not discussed here to remain within the scope of the work.

Furthermore, studies on deep rolling coupled with heat treatment and/or elevated temperature [73–76], cryogenic treatment [39,77], aging [56], and certain surface treatments like shot peening [78,79], burnishing [80], and ultrasonic-induced hammering [81–84] were testified in the recent past. The major objective was to complement DR with the advantages of the latter. However, it must be noted that they need to be performed with additional setups, involve complex process mechanics, and/or result in prolonged operating times.

Recently, in an innovative and novel work, P. Kuhlemann et al. [85] reported that the rolling temperature may be regulated through the appropriate selection and control of DR parameters. The rolling tool microgeometry and the rolling speed coupled with feed were

identified to be the key parameters that offered control over a wide range of temperatures (100 to 580 °C) for rolling AISI 1045 steel under stated conditions. The 3D FEM simulation approach was employed to establish the appropriate combination of process parameters to achieve an optimized rolling temperature, which was validated through experiments. In accordance with similar studies reported in the past [20,34,39], the said work revealed the significance of maintaining a constant temperature range during DR for achieving stabilized properties, which yielded greater fatigue lives. Their findings showed that increased tool nose radius and wear land width of the flank, reduced chamfer, and chamfer angle coupled with higher speed and feed significantly increased the process temperature, specifically in the surface/subsurface regions. In addition, surface roughness and tool wear were indicated to be the possible contenders for the further control of temperature. However, the detailed analysis of the same was stated to be a future scope. Nevertheless, the work established an effective methodology to regulate DR temperature through the control of process parameters. Further, A. M. Martins et al. [86] investigated in detail the in situ temperature development during DR and its influence on the attained surface/subsurface characteristics. Their study revealed that a rise in the process temperature was evident in response to changes in the control parameter magnitude. However, it was reported that the observed temperature rise during the DR process was not adequate to cause any significant structural changes; rather, the cold work was believed to be the sole reason for the attained surface/subsurface states. These deviations in findings between the two studies compared here accentuate the need for further scientific investigations to establish a definite conclusion on the role of temperature development during the DR process on the attained surface/subsurface properties.

Interestingly, there are a few recent studies focused on adopting novel measurement and/or characterization techniques for controlling the DR process. For instance, the wavelet transformation-based identification technique [87], the cos α-method of X-ray diffractometry with the micromagnetic approach [88], techniques for monitoring the surface quality [89], etc. These novel approaches indicate the potential for faster and more efficient control of the DR process in industrial applications.

Lately, numerous innovative and novel deep rolling techniques like pre-stress deep rolling [90,91]; diffusion with deep rolling [92,93]; turn-assisted deep rolling [94]; hard turning and deep rolling [95,96]; in-process semisolid deep rolling [97,98]; intermediate deep rolling in additive manufacturing [99,100]; and centrifugal force-assisted deep rolling [101] were reported. The major objective was to enhance the effect of conventional DR and/or reduce the processing time while ensuring similar benefits. The reported work demonstrates that these novel techniques certainly have an edge when compared with CDR. However, these complex systems are expensive and limited to certain applications, and their reliability is debatable.

Conventionally, DR was acknowledged for optimizing component properties, especially those involving high-stress applications. In contrast to this, recently, a few novel and innovative techniques employing DR for high-throughput material characterization, specifically for characterizing new construction materials developed based on micro-samples, were reported [102]. These studies unveiled that evaluating DR-induced plastic deformation and correlating it with mechanical properties could be an effective approach for high-throughput material characterization.

Furthermore, C. Schieber et al. [103] explored two process chain options involving laser machining and DR to compensate for the distortion effects arising in profile grinding. Their study involved extensive experimental and numerical analysis along with the development of an Artificial Intelligence (AI)-based model for predicting process chain control parameters to achieve optimized distortion compensation in AISI 4140 steel samples. The study is significant from the DR point of view, as it revealed the novel possibility of implementation of DR in commercial process chains for correcting machining-induced distortion.

The bulk of the studies pertaining to DR were on standard test specimens or similar components because of the obvious limitations of tooling and experimentation for application prototypes. Nevertheless, there are satisfactory efforts available on DR of components such as turbine/compressor blades [104–106], aircraft structural components [8,21], axels [107–109], shafts [110,111], crankshafts [112–114], tension bolts [115], high-strength fasteners and threaded parts [116,117], connecting rod screws [118], torsion bars [119,120], gear tooth [83], roller and thrust bearing race/rings [78,96,121], welded joints [122–126], blanking punch fillets [22], hip implants [26,27], etc. When deep-rolled, all these applications exhibited significant improvement in fatigue performance, which was attributed to substantial strain hardening, higher magnitude and deeper penetration of CRS, tailored surface region microstructure, and increased boundary layer hardness along with an improved surface finish. The prominent recent literature on the DR of steels is summarized in Table 4.

Table 4. Summary of the prominent recent literature on deep rolling of steels.

Author and Year	Materials, Process Parameters, etc.	Methods and Characterization	Key Findings
A. M. Abrao et al., 2014, 2015 [17,36]	Material: AISI 1060; Process: DR; Parameters: Rolling pressure/force, tool passes, ball diameter, and initial state of the material.	Experimental: Surface roughness, hardness, and CRS state and stability under cyclic loads.	• Initial state of the material, rolling pressure, and tool passes has the most significant influence. • The lower the initial material hardness, the higher the sensitivity to DR and better stability of the induced surface alterations under cyclic loading. • With increasing pressure and the number of tool passes, the ultimate strength increases, while the yield strength and surface roughness decrease. • Brittle fracture in treated samples.
D. Meyer and J. Kammler, 2016 [50]	Material: AISI 4140 steel; Process: DR; Parameters: Rolling pressure/force and ball diameter.	Analytical: Equivalent stress for estimating surface stress fields; Experimental: Residual stress state.	• Correlating the mechanism of DR, i.e., considering internal stress/strain could be viable option for better control over the process.
A. Tadi et al., 2017 [43]	Material: AISI 316L steel; Process: DR; Parameters: Rolling pressure/force, feed, and tool passes (15 and 26).	Experimental: Hardness and microstructure.	• DR is an excellent technique for inducing boundary layer grain refinement and strain-hardened martensitic structures. • Multiple passes yield a significant increase in surface hardness with deeper penetration and successfully induce a nano/ultrafine grain structure.
J. M. Cubillos et al., 2017 [42]	Material: AISI 304 and AISI 316 steels; Process: DR; Parameters: Rolling pressure/force, and feed.	Experimental: Surface roughness, hardness, residual stress state, and fatigue performance.	• Improvement in surface properties predominantly depend on rolling pressure, while the effect of feed on AISI 316 is insignificant. • AISI 304 shows superior HCF performance attributed to the formation of deformation twins and marginally higher martensitic phase.

D. Meyer and J. Kammler, 2018 [31]	Material: X210Cr12, X120CrMn5 and X150CrMn9 steels; Process: DR; Parameters: At constant rolling pressure, feed, speed, and ball diameter.	Analytical: Equivalent stress for estimating surface stress fields; Experimental: Surface hardness and phase.	• DR enables martensitic surface hardening. • Combination of hardening and finishing in one single step.
N. Lyubenova et al., 2019 [47]	Material: AISI 4140 steel; Process: DR; Parameters: Rolling pressure, number of tool passes, overlap percentage, pre-machining state, and measurement techniques.	Experimental: Residual stress state.	• Ambiguous conclusions indicating a high degree of interaction among the considered process parameters. • Control of the residual stress state is still a challenge.
P. R. Prabhu et al., 2015, 2020 [44–46]	Material: AISI 4140 steel; Process: DR; Parameters: Rolling ball material and size, rolling pressure/force, number of roll passes, initial surface roughness, coolant, feed rate, and speed.	Experimental: Surface roughness, hardness, residual stress state, fatigue performance, and corrosion resistance; Statistical: To establish the appropriate combination of parameters; Numerical: Residual stress states.	• A larger rolling force, larger ball diameter, and increased tool passes along with low initial surface roughness is identified to be the preferred combination. • DR is an effective surface treatment technique for realizing enhanced fatigue performance and corrosion resistance. • The use of statistical methods can be a feasible solution for dealing with highest level of uncertainties involved in optimizing DR process.
F. F. Do-Santos et al., 2021 [38]	Material: AISI 1020, AISI 1065, and AISI 1080 steels; Process: DR; Parameters: Impact of the carbon fraction, rolling pressure/force, tool passes, feed rate, and speed.	Experimental: Surface roughness, hardness, and microstructure.	• Rolling pressure is the most critical parameter; however, excessive pressures have adverse effects, which can be countered with carbon content • The feed rate set close to the prior machining operation deteriorated the surface, which was accompanied by increase in carbon content • In AISI 1080 steel, the surface hardness increased during DR, while it was unaffected/decreased for other two specimens. • Subsurface hardness increased in all cases; however, the affected depth decreased with carbon content • An increase in rolling pressure and roll passes caused higher grain deformation in low-carbon steels, while a larger speed and feed lessened it • In AISI 1080 steel, only an increase in the feed caused significant grain deformation, while all other parameters showed no/little effect.

A. M. Martins et al., 2022, 2023 [48,49]	Material: AISI 4140 steel; Process: Turning with subsequent DR; Turning Parameters: Depth of cut, feed, cutting speed; DR parameters: Rolling pressure, speed, feed, and turned surface state.	Experimental: Surface roughness, fatigue performance, fractography, microstructure, and microhardness; Statistical: To determine the parameter effect and establish the appropriate combination of parameters.	• DR significantly enhances the surface roughness and fatigue life of turned samples in most of the instances. • In specific cases, DR is not fully effective in eliminating the detrimental effects, particularly in the samples turned with higher feed rates. • The results indicate that previous machining parameters greatly influence the realized benefits from DR and thus, material in-service performance.

2.2. Finite Element Modeling of the Deep Rolling Process

The literature on DR process simulation through numerical methods is reviewed in this section to comprehend the approaches, modeling, applicability, and limitations. Since the time that some of the earliest studies were reported [127–130], the use of numerical methods, specifically FEM, to simulate the DR process has evolved significantly over the past three decades. However, the substantial research available is case-specific, and its universal adoption is often restricted. Nevertheless, the reported works indicate FEM could be an effective alternative for evaluating material responses with different process parameters over laborious experimental procedures.

J. Demurger et al. [131] discussed the applications (autofrettage, deep rolling, and bar straightening) in which control of the compressive residual stress field is vital and presented associated FE simulations. Deep rolling process simulations with the force control method were performed on 23MnCrMo5 steel crankshaft fillets with two hardening models including an isotropic hardening (linear) model and a nonlinear kinematic hardening (Lemaitre–Chaboche) model for comparison purposes. Their study revealed that a nonlinear kinematic hardening could not be ignored in FE modeling, especially for small cold deformation processes like deep rolling and, furthermore, in the case of cyclic loading. The authors emphasized that full 3D analysis is crucial for the efficient representation of the process and to predict the exact deformation path, albeit the achieved stress state was axisymmetric. However, the detailed process flow for simulation was not disclosed.

K. S. Choi and J. Pan [132] proposed a self-developed anisotropic hardening model for predicting the stress field in the rolling of crankshaft fillets and bending fatigue through FE simulation. Their study compared the model with the nonlinear isotropic–kinematic hardening model available in the FEA tool ABAQUS and validated it with experimental measurements. The reported 2D simulation results showed agreement with the nonlinear kinematic hardening model apart from compressive hoop stresses which were predicted to be higher and acknowledged experimental measurements.

G. H. Majzoobi et al. [133] assessed the effectiveness of SP and the DR process through experimental and numerical methods. However, the materials considered for experimental evaluation (Al7075-T6 alloy) and FE simulations (AISI 4340 steel) were reported to be different because of limited access to material data. Moreover, the numerical investigations were restricted to the comparison of induced stress levels and surface roughness because of modeling constraints. The Johnson–Cook elastic–plastic model was used to account for material deformation, while the roller was assumed to be rigid. The contacts between the mating surfaces were defined via automatic surface-to-surface contact in an ANSYS-LS DYNA solver. The results indicate that the depth and magnitude of residual stresses can be amplified through higher rolling force only up to a certain limit, which is governed by the yield strength of the material. A further increase in rolling force showed relaxation of induced stresses and depth; however, associated mechanisms were not discussed. It was indicated that a lower feed and a higher force could be preferred to

achieve a smoother surface finish. The study revealed that FE procedures can be successfully implemented for satisfactory prediction of surface roughness and induced stresses involved in mechanical surface forming processes like SP and DR.

In another work, G. H. Majzoobi et al. [60] investigated the effect of DR process parameters (rolling force, rotational speed, number of passes, roll size, and roll feed rate) on Al7075-T6 material characteristics through experimental and numerical methods. Three-dimensional FE simulations were performed through the ABAQUS explicit dynamics module. A small sector of an axis-symmetric geometry was assumed to be a deformable body attributed to the Chaboche cyclic plasticity model, while the roller was considered to be rigid. Their findings showed that the DR effect was predominant in the high-cycle fatigue regime, while in the low-cycle fatigue regime, it was observed to be negligible. Among the considered parameters, rolling force/pressure showed a pronounced effect on residual stresses, while a slower feed rate demonstrated increased CRS depth. The smaller size ball induced a uniform stress distribution, while the larger size ball resulted in an increased CRS. However, the penetration depth was reported to be unaffected. Unfortunately, appropriate clarifications of these observations were not reported.

V. Backer et al. [134] analyzed the effect of DR on a Ti-6Al-4V alloy turbine blade through FE modeling. To realize the material behavior through simulation, the DR process was modeled as a sequence of small successive forming processes with the nonlinear combined isotropic–kinematic strain hardening law available in the ABAQUS FEA tool. In addition, the linear elasticity model was considered to determine the elastic nature of the material. The rigid ball tool kinematics were defined via force control for depth penetration and displacement for in-plane translations. For FE modeling a small portion of the whole structure with appropriate boundary conditions to define surrounding material was accepted, owing to practical limitations with FEA and assuming DR affects only near-surface regions. However, it was reported that with these assumptions, a compromise in accuracy was inevitable, especially for thin-walled structures like turbine blades, where rolling parameters can result in deformations of the entire geometry. Therefore, the authors suggested coupled Finite Element and Boundary Element (FE-BE) analysis, which complements each other for efficient prediction of material behavior. Their study revealed that coupled FE-BE analysis could be a potential alternative for global modeling of the DR process to achieve a considerable reduction in computation time with accuracy on par with FEA.

M. Salahshoor and Y. B. Guo [53] investigated the process mechanics involved in deep rolling Mg-Ca biodegradable alloy through experimental and FE simulation techniques. The primary aim of the FE simulation was to estimate elastic recovery after rolling, which was reported to be difficult to predict through physical inspection. In addition, the dent geometry, temperature with induced residual stresses, and strains were investigated. The internal state variable (ISV) plasticity model available in the ABAQUS FE tool was used to model the dynamic behavior of the material, while the rolling ball was modeled as rigid. The 2D simulations were performed with axisymmetric boundary conditions at the edge near the tool interaction, while to allow stress waves to propagate through a non-reflective boundary, quiet boundary conditions were employed for semi-infinite elements at farther edges. Experimental and FE results showed a similar nature but a fair deviation in magnitude that was attributed to limitations with 2D modeling. It was reported that the elastic recovery, which is inevitable in plastic deformation processes like DR, increased with increased loads, albeit the reasons for the same were not identified. The results showed a minor variation in operating temperature, which indicates that the DR process may be considered an isothermal process. Unfortunately, in the said work, the DR process was restricted to a point over a surface, which indicates that the obtained results may not be comparable with practical applications where DR of the entire surface is required.

A. Manouchehrifar and K. Alasvand [135] performed a 3D simulation of the DR process on a Ti-6Al-4V alloy flat geometry model using the ABAQUS FE tool. The influence of DR parameters (overlap, friction coefficient, rolling force, and force variation due to the

spring-back action of the tool) on induced residual stresses was analyzed. The material behavior was modeled using the Johnson–Cook elastic–plastic model, while the roller was modeled as a rigid body with concentrated mass at the center. It was demonstrated that an increase in the overlap and rolling force showed a larger residual stress field, while an increase in friction coefficient showed an adverse effect. Moreover, the spring-back action force, which is more practical in DR operations, induced a higher CRS than with constant load simulations. However, appropriate elucidations for these observations were not detailed and/or not validated through experiments.

G. Nicoletto and A. Saletti [136] analyzed the role of DR-induced residual stresses on the fatigue life of notched 30NiCrMo12 steel specimens through experiments and FE simulations. The simulations were performed with a symmetry in geometry assumption for containing the computational time with an elastic–plastic material deformation model through the ABAQUS explicit module. Unfortunately, details of the FE procedures implemented were not disclosed. However, the presented FE modeling process was claimed to deliver reasonable agreement with measured parameters within the stated assumptions.

J. J. Liou and T. I. El-Wardany [137] investigated residual stress states in Ti-6Al-4V alloy plate through numerical simulation of the DR process involving complex roller paths. The 3D FE simulations were performed through ABAQUS with the explicit dynamic technique. The material kinematic hardening/softening behavior during loading/unloading was modeled through the elastic–plastic Johnson–Cook (JC) material model. This model was reported to be extensively adopted for predicting material flow under a high strain rate along with operating temperature consideration with proven confidence, albeit it assumes isotropic strength and an empirical nature. The interaction between the rigid roller tool and the deformable plate was modeled through Coulomb's law with free rotation of the tool, highly lubricated, and isothermal rolling assumptions. The FE model was reported to be validated in two ways including an analytical method using Hertzian contact theory and experimental results available in the literature. However, the validation involved a comparison with simple roller path conditions, and the authors encouraged further validation with complex roller path conditions to realize the scope of the developed model fully. In contrast to most of the studies that indicate a uniform CRS distribution, their study showed a non-uniform distribution of induced residual stresses in surface/subsurface layers and turned into a tensile nature, especially at the edges of the rolled path. This was attributed to the combined effect of micro-slip arising because of the close conformity of the filleted roller end with rolling track boundaries and the translational motion of the roller, which caused an offset in the assumed complex roller path.

K. Kumar et al. [138] studied the effect of DR controlling parameters (rolling ball diameter, rolling force, number of rolling passes, and initial surface roughness) on induced residual stresses in AISI 4140 steel material through 2D explicit dynamic analysis in the ANSYS/LS-DYNA module. In addition, a two-level fractional factorial design using DOE was employed to reduce the number of simulations. A Cowper–Symonds isotropic–kinematic hardening model with strain rate dependency was employed to model material behavior. The displacement method to control the ball movement was reported to be appropriate for 2D simulation, while the force control method was found to underestimate the penetration depth of the ball within the assumed conditions. Moreover, the work emphasized the use of an appropriate contact definition for mating surfaces and preferred surface-to-surface contact, while the effect of the friction coefficient was reported to be negligible. The results showed that all the considered parameters had a significant influence on the estimated stress state within the assumed conditions. However, the deviations observed (about 15%) in comparison with experimental measurements were attributed to limitations with 2D modeling. This indicates the need for detailed 3D simulations to realize the effect of the DR process fully. Interestingly, the initial surface roughness parameter considered in their study, which significantly influenced the computed stress field, was not considered in most of the similar research reported so far. Unfortunately, the residual

stress fields reported were restricted for the direction of applied rolling force, which does not rationalize the role of induced stresses fully with practical applications.

A. Lim et al. [139] investigated the effect of the friction coefficient on the achieved residual stress state through a full 3D FE simulation of the DR process on Ti-6Al-4V alloy using the ABAQUS tool. It was reported that the friction coefficient had minimal impact on the estimated residual stress state and negligible influence beyond 0.4 mm of depth. However, it was noted that a difference existed in the computed stress state with frictionless conditions and cases with friction, which made considering a small value of friction coefficient imperative for efficient modeling. This was attributed to the free rotation of the tool condition in the DR process, which required some level of friction to purely roll instead of sliding over the component surface.

Furthermore, in their extended work, A. Lim et al. [67] predicted the effect of DR on the induced stress field through FE simulations and validated t with experimental results. Regular cuboidal geometry was modeled as an elastic–plastic deformable body with strain hardening. The rigid rolling ball kinematics were regulated via force control for depth penetration (assumed to remain constant during simulation) and displacement boundary conditions for in-plane translations. In contrast to most akin studies that recommended the use of an explicit dynamics solver, the reported work used an implicit Newtonian solver assuming a quasi-static process that used higher-order terms while estimating strains to account for geometric non-linearity. The findings showed that the predicted and measured stress fields exhibited adequate correlation, which indicated that the reported FE modeling approach could be adapted within the stated conditions.

S. M. Gangaraj et al. [140] proposed a more realistic FE model to overcome some of the reported shortcomings in the simulation of DR. Extensive FE investigations on the role of DR process control parameters, namely, rolling pressure, rolling feed, roll geometry, and coverage of the roll on the induced residual stress state in EA4T steel railway axels, were presented with authentication through experiments. In addition, parametric studies were performed to arrive at an appropriate combination of controlling parameters through DOE. A 3D FE model of the deformable body subjected to force-controlled analytically rigid ball penetration was analyzed through the ABAQUS explicit dynamics module. The cyclic stress–strain data obtained through experiments were utilized as input for modeling material behavior assuming the von Mises criterion for yielding, isotropic hardening, no hardening at severe plastic strains, and frictionless tangential surface contact over a flat target surface. Their findings showed that higher loads, lower feeds, and larger roll sizes, all of which resulted in increased coverage, could be the ideal choice. However, too-high coverage showed a detrimental effect, which indicated that recognizing the optimum range is crucial to realize the benefits of DR fully. Roll coverage was believed to be the single master parameter for fully controlling the effect of DR.

N. Lyubenova and D. Bahre [23,141] extensively investigated the reliability of finite element modeling in estimating the residual stresses in AISI 4140 steel and reported the effect of variation in control parameters on the computed results through 3D explicit dynamics simulation in ABAQUS v6.14. Four different material models (elastic perfectly plastic, isotropic-plastic, bi-linear kinematic hardening, and Johnson–Cook models) with different combinations of controlling parameters (rolling pressure, number of passes, and percentage overlap) were considered in the study. It was reported that the use of a bi-linear kinematic hardening model or the Johnson–Cook model over other options achieved a better approximation of the results, albeit the authors identified cautions about the obvious limitations in modeling non-linearity, which was observed in the physical process of material deformation. The simulation demonstrated that an increase in rolling pressure induced higher magnitude and deeper penetration of residual stresses, while the number of passes prompted an increase in only penetration depth, which was reported to be in accordance with the experimental behavior within the assumed conditions. However, with the partial overlapping of passes (25, 50, and 75%), no or little relaxation in induced stresses was observed, which is in contrast to experimental indications where

significant relaxation was reported. In addition, no overlap and the 100% overlap simulation did not yield the expected outcomes, which were attributed to limitations with modeling. The study illustrates the potential of FE modeling for efficiently predicting anisotropy in induced stresses and concludes that selecting the appropriate material model is crucial in achieving the reliable computation of residual stresses through simulation and evidencing with experiments is a must.

J. Perenda et al. [119] simulated the DR process on a TORKA steel (similar to AISI 4340 steel) torsion bar with the intention to evaluate the residual stresses and compare them with experimental measurements. The authors emphasized the need for the FE modeling of the DR process because of the significant influence of a large number of process parameters on the material/component characteristics, especially residual stresses for which experimental verification is cumbersome and expensive. However, it was noted that the FE modeling of the DR process is complex, and the accuracy attained is sensitive to modeling approaches. For this reason, the reported simulations were conducted on a small portion of the workpiece assuming the DR process introduces uniform deformation across the entire surface layer and induces large strain gradients only in near-surface regions. The process was simulated through an explicit dynamics algorithm with the master–slave contact penalty method and a non-linear kinematic model (Lemaitre–Chaboche model) was used to model material behavior. The influence of symmetry boundary conditions for an axis-symmetric section was reported to be negligible. However, the size of the workpiece section modeled was reported to have a significant influence on the computed results, especially on the computed stress field. The study showed that input parameters of the DR process have a significant impact on the final level of the induced residual stresses, which makes the careful selection of modeling parameters imperative. Interestingly, the study revealed that the depth and distribution of the equivalent plastic strain observed through simulation and experimentally measured FWHM values were nearly identical. These reported findings indicate that a correlation could be established with equivalent plastic strain to estimate the depth of work-hardened/-softened layers.

V. Zaharevskis et al. [142] identified hardening quality as a reliable parameter to recognize the influence of DR on service properties of materials/components. It was stated that effective control of hardening quality, which is defined via uniformity, thickness, and residual stresses developed in the hardened zone during DR is still a concern. This was believed to be due to several process control parameters (rolling load, tool shape and size, number of passes, rolling speed, etc.) and manufacturing factors (interaction of the tool and workpiece profile/geometry, tool wear, etc.). The rolling process simulated through the MSC Marc and Mentat FE tool was validated with ring-cut method experiments. Their findings showed that the manufacturing factors considered had adverse effects on hardening quality, which indicated that for efficient rolling, the tool and workpiece surfaces must be in uniform contact. Interestingly, the ring-cut method proposed in their work was observed to be an economical and effective method for assessing hardening quality and subsequent parameter optimization of the DR process.

D. Mombeini and A. Atrian [59] studied the effect of DR parameters (rolling depth, feed rate, number of passes, ball diameter, and friction) on induced stress states in C38500 brass material through 2D FE simulations using the ABAQUS tool and correlated the results with experimental data. The simulation results showed that increasing the rolling depth/force enhanced the CRS magnitude and depth. However, the experimental measurements did not verify the same, which was attributed to an inability of the FE model to mimic the practical material behavior where microcracks arise at higher loads. Furthermore, an increase in ball diameter induced higher stress amplitudes with higher depth penetration, which was thought to be due to the larger contact area resulting in larger contact forces. However, it was observed that the larger contact area created tensile residual stresses in the surface and a few layers below before transitioning into compressive nature, which was reported to be due to the material being pulled during rolling. In addition, lower feed rates coupled with multiple roll passes were reported to be beneficial.

T. Kinner-Becker et al. [143–145] extensively investigated the internal material loads and residual stress fields generated during DR in AISI 4140 steel through FE simulation using the ABAQUS tool. Both types of simulations using quasi-static implicit and explicit approaches along with the Chaboche nonlinear kinematic hardening material model were performed. The results were also validated through experiments. Their findings showed that FE modeling can be employed for effectively simulating multi-step DR processes and predicting material response (i.e., internal material loads and residual stresses). In addition, it was reported that the initial stress state of the material has minimal impact under assumed conditions and thus, may be neglected in FE modeling. Further, they revealed that the concept of *process signatures* may be successfully employed for inversely determining the appropriate DR process parameters to achieve desired residual stress fields. This appears to be a significant finding, as it aids control of the DR process, especially in practical applications without performing laborious process optimization studies.

K. Han et al. [69] performed both 2D and 3D FE simulations with the ABAQUS 6.13v tool in order to investigate the effects of deep rolling parameters on residual stress states in Ti-6Al-4V material. The Chaboche nonlinear kinematic hardening material model was employed to model the assumed material behavior. The study revealed that 3D simulations yielded more accurate results than 2D simulations as the former represents practical conditions better. The simulation results indicated that DR process parameters like, rolling pressure, tool overlap, rolling speed, rolling ball diameter, and the number of tool passes significantly affected the residual stress profiles. The effect of the friction coefficient was observed to be minimal. It was reported that these findings were validated through experiments and thus indicate the potential of established FE simulation methodology for the accurate prediction of DR-induced residual stress fields.

J. Bialowas et al. [146] proposed a general FE methodology to simulate the deep rolling process on the sector of cylindrical components similar to part of a railway axel. The simulation involved modeling cyclic material behavior through simplified geometry conditions and implementing coupled boundary conditions along with shadow elements. In contrast to most of the available studies that use an explicit dynamics module, they considered the implicit FE model in the commercial ABAQUS FEA tool. The FEA methodology developed was reported to be efficient for yielding faster simulation with higher accuracy of results.

Some application-specific studies involving the simulation of DR of crankshafts [114,147,148], railway axels [109,149], cylinder inner surfaces [80,150], fine blanking punch edges [22], turbine/compressor blades [105,134], torsion bars [120], and welded joints [124,126,151] revealed the potential of numerical techniques for effective assessment and optimization of process parameters. However, the material models and boundary conditions along with process kinematics were reported to be the key factors that must be modeled appropriately to obtain a reliable conclusion. In addition, it was stated that full-scale numerical analysis may not be feasible because of limitations involved with modeling the complex nature of process kinematics coupled with a large computational time and/or cost. Therefore, the studies reported were mostly restricted to predicting induced residual stress states with reduced model size and modified boundary conditions. Nevertheless, FE modeling was identified to be the effective alternative for initial approximations within the assumed conditions, and further validations could be achieved through a limited number of experiments with optimized parameters. The prominent recent literature on the finite element modeling of the deep rolling process is summarized in Table 5.

Table 5. Summary of the prominent recent literature on finite element modeling of the deep rolling of steels.

Author and Year	Materials, Process, Parameters, etc.	Methods and Characterization	Key Findings
K. Kumar et al., 2014 [138]	Workpiece: AISI 4140 steel, elastic–plastic deformable body, Cowper–Symonds model. DR Tool: Ball, rigid body, revolves about the axis and translates. FEA tool: ANSYS LS-DYNA explicit dynamics module.	Simulation: 2D, displacement-controlled. Parameter: Residual stress state, surface roughness. Validation: experimental results.	• Rolling force, ball size, tool passes, and initial surface roughness parameter significantly influence the computed stress field. • Plane strain condition assumption does not fully correlate with measured values.
S. M. Gangaraj et al., 2015 [140]	Workpiece: EA4T steel, elastic–plastic deformable body, JC model. DR Tool: Roller, rigid body, revolves about the axis and translates. FEA tool: ABAQUS, explicit dynamics module.	Simulation: 3D, load-controlled. Parameter: Residual stress state. Validation: Experimental results.	• The parameters that aid in increased coverage can be the ideal choice; however, too-high coverage leads to detrimental effects. • Roll coverage appears to be the single master control parameter.
J. Perenda et al., 2016 [119]	Workpiece: TORKA steel, elastic–plastic deformable body, LC model. DR Tool: Roller, rigid body, revolves about the axis and translates. FEA tool: ABAQUS, explicit dynamics module.	Simulation: 3D, load-controlled. Parameter: Residual stress state, equivalent plastic strain. Validation: Experimental results.	• FE modeling can be a viable option for analyzing CRS; however, minor deviations from the measured values are unavoidable. • An appropriate portion of the workpiece needs to be modeled for satisfactory simulation. • Equivalent plastic strain obtained through simulation were identical to the measured parameters.
N. Lyubenova and D. Bahre, 2017 [141]	Workpiece: AISI 4140 steel, elastic–plastic deformable body, four different material models. DR Tool: Ball, rigid body, revolves about axis and translates. FEA tool: ABAQUS 6.14v, explicit dynamics module.	Simulation: 3D, load-controlled. Parameter: Residual stress state. Validation: Experimental results.	• A bi-linear kinematic hardening model or the JC model can be preferred options. • An increase in rolling pressure induces a higher and deeper CRS state, while the number of tool passes only increases the penetration depth. • FE modeling can efficiently predict anisotropy in induced stresses.
V. Zaharevskis et al., 2018 [142]	Workpiece: Material not specified; deformable condition modeled with stress–strain data, revolves about axis. DR Tool: Roller, rigid body, revolves about the axis and translates. FEA tool: MSC Marc and Mentat.	Simulation: 3D, load-controlled. Parameter: Hardening quality. Validation: Ring-cut method experimental results.	• Manufacturing factors have adverse effects, which indicate that for efficient rolling, the tool and workpiece surfaces must be in uniform contact. • The ring-cut method appears to be an economical and effective method for validating FE results.
T. Kinner-Becker et al., 2020, 2021,	Workpiece: AISI 4140 steel, deformable body, Chaboche nonlinear kinematic hardening material model.	Simulation: 3D, both load- and displacement-controlled.	• FE modeling can be effectively employed for simulating a multi-step DR process and predicting the

2023 [143–145]	DR Tool: Ball, rigid body, revolves about the axis and translates. FEA tool: ABAQUS, quasi-static implicit and explicit approaches.	Parameter: Residual stress state, equivalent plastic strain. Validation: Experimental results.	material response (i.e., internal material loads and the residual stresses). • The concept of *process signatures* may be successfully employed to inversely determine the appropriate DR process parameters to achieve the desired residual stress fields. • The initial stress state of the material has minimal impact under assumed conditions and thus may be neglected in FE modeling.
J. Bialowas et al., 2023 [146]	Workpiece: Railway axel material, cyclic material behavior, combined isotropic–kinematic hardening material model. DR Tool: Roller, rigid body, revolves about the axis and translates. FEA tool: ABAQUS, implicit analysis with periodic boundary conditions.	Simulation: 3D, load-/displacement-controlled. Parameter: Residual stress state, equivalent plastic strain, FE computation time. Validation: Not reported.	• A general FE simulation procedure for the deep rolling of cylindrical component is proposed. • Faster simulation and higher accuracy of the predicted results is achieved through proposed method.

2.3. Deep Rolling Tools

The literature on DR tools is reviewed in this section to understand the aspects of tool design and construction details. Consistent efforts by the research community are observed on tool designs for the DR of crankshafts and/or similar symmetrical mechanical components fillets, radii, and recesses. However, a significant amount of the work is patented. Most designs involve tool assembly with ball or roller elements in horizontal, vertical, or inclined positions depending on the application. The contact mechanics of the tool tip with the workpiece, degrees of freedom of the rolling ball, the ability to maintain constant rolling pressures, and the mechanism of applying rolling force are acknowledged aspects of tool design.

C. C. Wong et al. [21] investigated the effectiveness of three types of DR tools (a single-roller tool, a caliper ball tool, and a double-roller tool) on various geometrical features. The study revealed that the selection of an appropriate tool based on geometry is a must for achieving the desirable level of surface alterations.

A. M. Abrao et al. [152] summarized several mechanisms developed for steadily holding a ball/roller against the workpiece and discussed their selection criteria. The schematic of well-established tool designs reported is presented in Figure 7. The tools with a hydrostatic pressure mechanism (Figure 7a) were often used in applications where steady and higher rolling pressures were required. Moreover, fewer kinematic pairs coupled with self-lubrication by the hydraulic fluid minimizes the energy loss due to friction. However, they were quite expensive. The other category of tools primarily uses mechanical elements like springs or threaded bolts for generating rolling pressures. Several variations involving the mechanism to hold the ball/roller were reported, as depicted in Figure 7b–e. Though they were cost-effective when compared with the former, obvious limitations like friction, degrees of freedom at the tool tip, vibrations especially at higher rolling loads, and pressure variations during rolling resulted in inconsistent modification of material properties.

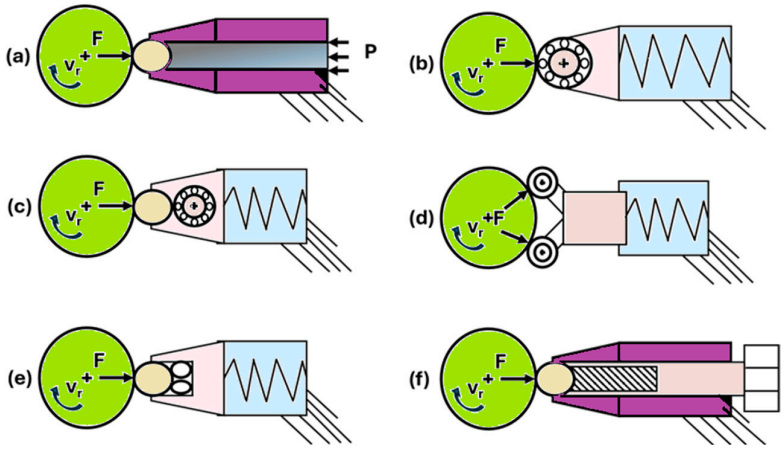

Figure 7. Schematic of the working mechanisms for deep rolling tools [152]. (**a**) Hydrostatic pressure, (**b**) bearing supported by a spring, (**c**) ball supported by an intermediate bearing and spring, (**d**) two bearings supported by a spring, (**e**) three-ball assembly supported by a spring, and (**f**) a ball supported by a bolt adopted with ref. [152] SPRINGER 2014.

P. R. Prabhu et al. [153] proposed two tool designs with mechanical loading mechanisms involving springs (Figure 8a) and threaded shanks (Figure 8b) for the DR of steel material. From their work, it is evident that despite the obvious advantages like better control over the rolling force and the absorption of shock with the spring mechanism for the tool, it was unable to withstand high rolling loads because of limitations with spring stiffness. Alternatively, a design with a threaded shank mechanism was identified to be better to sustain high rolling loads, especially when used for hard materials like steel. However, the relative motion of the rolling ball in contact with the workpiece was confined to certain axes because of the limitations of ball seating arrangements.

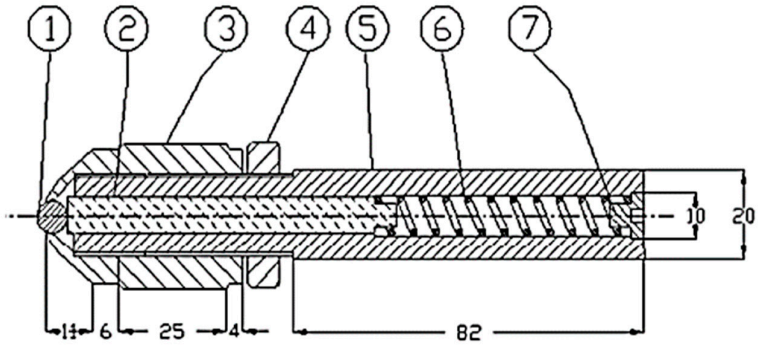

1 – Rolling ball, 2 – Hardened pin, 3 – Collet (Adapter), 4 – Locking nut (counter nut)

5 – Shank, 6 – Spring, 7 – Allen screw

(**a**) Push rod and spring mechanism

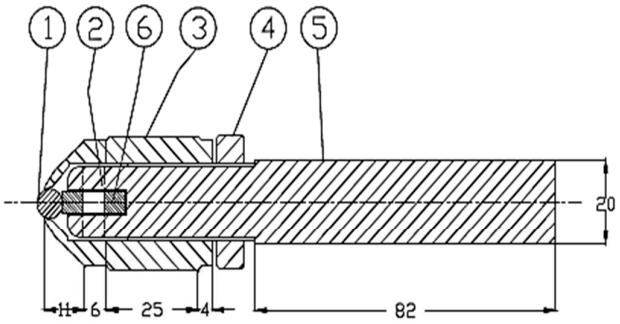

1 – Ball, 2 – Hardened pin, 3 – Collet (Adapter), 4 – Locking nut (counter nut)

5 – Shank, 6 – Bearing

(**b**) Threaded shank with intermediate roller

Figure 8. Schematic of deep rolling tool mechanisms reprinted with permission from author ref. [153], PhD thesis, Manipal University, Manipal, 2014.

M. Gryadunov et al. [80] presented a tool to perform simultaneous DR and burnishing hollow cylindrical parts like bush-bearing surfaces over the lathe. The tool consisted of three equi-spaced steel rollers—one for inducing DR deformation and two for burnishing—which were fitted in a cylindrical cage. The DR roller was provided with chamfer and fillets to ensure a higher penetration than the latter. All the rollers were made conical in shape to regulate the indentation depths and were able to freely rotate about their own axes and about the device axis. This tool ensured consistent forces on the work surfaces, thus developing the intended surface/subsurface characteristics.

J. M. Cubillos et al. [42] developed a tailored device for deep rolling based on a spring-loaded ball element, as shown in Figure 9. However, exact design details were not reported. Thus, it is not clear which mechanism they used to hold the ball at the tool tip with the antifriction element, which governs the degrees of freedom imparted to the ball.

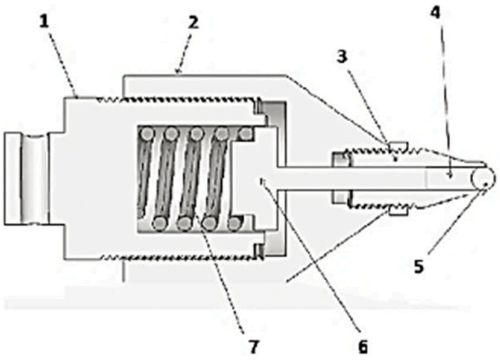

1. Lower body.
2. Upper body.
3. Nozzle.
4. Antifriction element.
5. Ball (ϕ10 mm).
6. Support of spring and pushing element.
7. Spring.

Figure 9. Sectional view of the deep rolling device used reprinted with permission from ref. [42] ELSEVIER 2017.

S. Sattari and A. Atrian [70] modified the tool design presented earlier in Figure 7f by incorporating an additional intermediate ball (Figure 10) between the rolling ball and the force-inducing bolt. This altered design ensured relative motion between the rolling ball and the workpiece, which is crucial for efficient DR. A summary of key aspects found in the literature reviewed here on DR tools is presented in Table 6.

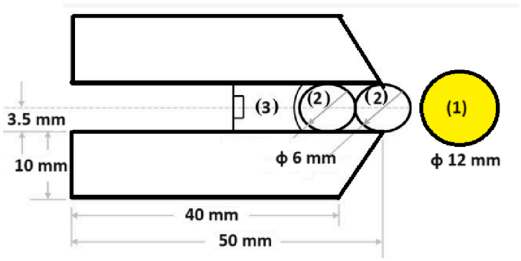

Figure 10. Schematic of the deep rolling tool used in 1—specimen, 2—rolling and support balls, 3—Allen bolt adopted with ref. [70] SPRINGER 2017.

Table 6. Summary of the prominent recent literature on deep rolling tools.

Author and Year	Key Findings
C. C. Wong et al., 2014 [21]	• Selection of an appropriate tool shape must be based on workpiece geometry for achieving desirable surface alterations.
A. M. Abrao et al. 2014 [152]	• Hydrostatic tools are often used in applications where steady and higher rolling pressures are required; however, they are expensive and involve a complex mechanism. • Tools with mechanical elements like springs or threaded bolts for generating rolling pressures could be an economical option. • Friction, the degrees of freedom at the tool tip, and vibrations at higher rolling loads must be carefully controlled for consistent rolling operation.
P. R. Prabhu et al. 2014 [153]	• Tools with a spring mechanism may not withstand high rolling loads owing to limitations with spring stiffness. • Tools with a threaded shank mechanism could better sustain high rolling loads.
S. Sattari and A. Atrian, 2017 [70]	• The design developed ensured free relative motion between the rolling ball and the workpiece, which is crucial for efficient DR.

2.4. Roll of ANNs in Deep Rolling Techniques

The Artificial Neural Network (ANN) is based on the human brain's neural structure for processing information through interaction with multiple neurons and is an established technique in several industrial applications. However, the adoption of ANN specifically for predicting deep rolling effects is not available in the open domain to the best knowledge of the authors of this review paper. Nevertheless, few studies are available on the implementation of ANNs for predicting the effects of burnishing, which is a similar process to that of deep rolling in principle and at least with that of attained surface topography [154–157].

Esme et al. [154] adopted the ANN technique for the prediction of surface roughness attained through ball burnishing. They modeled an ANN considering burnishing force, speed, feed, and the number of tool passes as input parameters while modeling surface roughness as the response output. A supervised learning approach through MATLAB programming was used to train the system. The work revealed a close prediction of average surface roughness through ANNs with that of experimental outcomes. This indicates that ANNs could be effectively applied for predicting burnishing process responses.

Tang et al. [155] used the ANN technique to predict the friction coefficient in the roller burnishing process for two different roller orientations. The roller curvature, burnishing speed, and force were considered as input parameters. They performed extensive work involving 60 variations of ANN configurations, which were trained using six

different algorithms with large data sets for training and testing. The results obtained were reportedly close to the experimental data, which proved the efficient adoption of ANNs for the prediction of the friction coefficient under the derived conditions. Furthermore, the authors acknowledged that the architecture of the ANN is the key aspect in the satisfactory prediction of response, which demands problem-specific cautious selection and design of the ANN configuration.

Kluz et al. [156] reported the use of ANNs for the prediction of surface roughness of shafts in slide burnishing. They indicated that ANNs are more effective in comparison with multiple responses, multiple regression, or Taguchi analysis because of the availability of multiple links in neural structure. Their results indicated the effectiveness of ANNs in predicting surface topography variation in slide burnishing. In addition, the work also highlighted the possibility of ANNs to predict outputs beyond a certain range by increasing the input parameter range and the number of training sets.

Nguyen et al. [157] used ANN techniques to predict the effect of lubrication during the roller burnishing process on the attained surface characteristics, namely, the maximum height of surface roughness and hardness. Unlike other studies reviewed here that involved primary burnishing factors as input parameters, their work is assumed to be the first that focused on developing an ANN model for predicting the effect of Minimum Quantity Lubrication (MQL) burnishing. The input parameters considered were only the MQL control factors. The developed ANN configuration demonstrated agreeable prediction with that observed through experiments, which proved the effectiveness of the technique under the assumed conditions. In addition, the work reported a significant influence of MQL control parameters on the investigated surface properties, which is often neglected in most of the works.

3. Conclusions and Scope for Further Study

The conclusion drawn from this review underscores the complexity of establishing generalized standardizations for the deep rolling process. It emphasizes the necessity for specific optimization studies tailored to the material in question because of the intricate interplay of controlling parameters. Despite the significance of the deep rolling process, the literature concerning the characterization of surface and subsurface properties of deep-rolled AISI 1040 steel, as well as the optimization of process parameters, remains limited.

- The literature indicates there are reliable efforts by the research community in developing the DR process, optimizing the process parameters, and studying its effect on materials or components with an objective to achieve improved in-service performance. Conversely, comparative studies on the effect of various MSTs are scarce, which could be due to the significant differences involved in the process mechanisms/parameters and their effect on the performance of the component/material. This includes, for instance, different stability and heterogeneity in induced CRS, cold work and microstructures, different responses of different metallic materials to residual stresses and mean stresses, different work-hardening capabilities, different mechanical or complex thermo-mechanical responses under cyclic load, during MSTs at elevated temperatures, etc.
- The literature in the open domain reveals that DR could be the most viable option because of its simple operation and tools, lower cost, and the highest level of beneficial surface properties when compared with contemporary techniques. It is identified to be one of the most effective commercially available methods to enhance the fatigue performance of metallic materials because of the remarkable improvement in surface finish, significant CRS depth up to 3 mm (material- and process parameter-dependent) with work-hardened microstructures, and directional strength enhancement.
- The reviewed literature demonstrates that standardizing the DR process is a quite challenging aspect considering the highest degree of influence of process parameters

(rolling force/pressure, rolling feed, tool geometry size and material, number of roll passes, coverage/overlap of the rolling path, contact conditions, etc.) on the material or component performance. Moreover, the type and initial condition of the material are crucial in achieving desirable properties through DR. For instance, too-low rolling pressures might not induce pronounced benefits, while too-high rolling pressures might deteriorate the existing properties by inducing micro-cracks. This indicates that each study is unique and necessitates the requirement of material-specific investigation with optimized parameters to fully realize the benefits of the DR process.

- The reasonable literature recommends considering physical and mechanical characteristics (microstructure, surface topology, hardness, CRS, and cold work) over the use of empirical methods for process parameter optimization.
- Significant research on the use of FEM to simulate the DR process and analyze its effect on the material/component is available in the open domain. However, a substantial amount of the research available was observed to be case-specific, and its universal adoption is often restricted. In addition, the simulation and accuracy achieved were sensitive to variations in modeling techniques and assumed boundary conditions, which were reported to be the primary reason for the deviation among computed and measured parameters.
- Most of the conveyed FE studies are focused on the evaluation of DR-induced residual stress fields. In contrast, the use of FEM for predicting elastic recovery, surface roughness, accumulated plasticity, and fatigue life in DR specimens is quite rare. The reviewed literature indicates that DR controlling parameters, namely, the friction coefficient, rolling pressure, number of rolling passes, rolling path and overlap, roller shape and size, and surface roughness, could be the preferred input parameters in FE modeling.
- The literature on DR tool design and developments divulges that most of the work is patented. The reviewed literature emphasizes the contact mechanics of the tool and workpiece, degrees of freedom of the rolling ball, and the ability to maintain constant rolling pressures were critical aspects in tool design. Limited organizations, especially in India, are involved in the development and manufacturing of DR tools. Most of the business is restricted to the development and marketing of burnishing tools. In addition, the available tools are developed for specific applications and are fairly expensive.
- Investigations on mechanical surface treatments of AISI 1040 steel are scarce in the literature. The available work is mostly restricted to burnishing, peening (shot/liquid jet), and laser surface treatments. In particular, no plausible studies pertaining to the DR of AISI 1040 steel have been reported in the published domain so far.
- The adoption of ANNs specifically for predicting deep rolling effects is not available in the open domain for AISI 1040 steel.

This study identified several areas that require additional research after an assessment of the current literature including the following:

- Establishing generalized standardizations for the deep rolling process does not appear to be feasible because of the multiple controlling parameters and their complex interactions. This necessitates a specific optimization study corresponding to the material of interest for process standardization.
- Investigation studies on the characterization of surface and subsurface properties of deep-rolled AISI 1040 steel and process parameters optimization are limited in the published literature.
- Detailed investigations on the microstructure and the interaction of surface/subsurface properties in deep-rolled samples are meager.
- Numerical, analytical, statistical, and ANN studies are limited in comparison with experimental work on the deep rolling process.

Author Contributions: Conceptualization, D.J.N., S.S., R.P.P. and G.S.; methodology, R.P.P.; software, S.D. and N.K.; validation, D.J.N., S.S., S.D. and R.P.P.; formal analysis, G.S., N.K. and R.P.P.; investigation, D.J.N., N.K. and S.D.; resources, R.P.P.; data curation, D.J.N. and S.D.; writing—original draft preparation, D.J.N., S.D. and R.P.P.; writing—review and editing, D.J.N., R.P.P. and N.K.; visualization, S.S. and G.S.; supervision, R.P.P. and G.S. All authors have read and agreed to the published version of the manuscript.

Funding: This research received no external funding.

Conflicts of Interest: The authors declare no conflicts of interest.

Abbreviations

AISI	American Iron and Steel Institute
ASTM	American Society for Testing and Materials
ANN	Artificial Neural Network
BSs	British standards
CDR	conventional deep rolling
CRS	compressive residual stresses
DIN	Deutsches Institutfür Normung e.V. (German Institute for Standardization)
DR/DCR	deep rolling/deep cold rolling
DR-CT	deep rolling at cryogenic temperature
DR-ET	deep rolling at elevated temperature
DR-RT	deep rolling at room temperature
ENs	European norms (European standards)
FE	finite element
FEA	finite element analysis
FEM	finite element method
FWHM	full width half maximum
HP	hammer peening
HT	heat treatment
HT + DR	heat treatment with deep rolling
IS	Indian standards
JIS	Japanese industrial standards
LSP	laser shock peening
MSET	mechanical surface enhancement technique
MSP	micro-shot peening
MST	mechanical surface treatment
PP	Piezo peening
SAE	Society of automotive engineers
SP	shot peening
UDR/USR	ultrasonic deep rolling/ultrasonic surface rolling
USP	ultrasonic shock peening
WP	water peening
XRD	X-ray diffraction

References

1. Matlock, D.K.; Alogab, K.A.; Richards, M.D.; Speer, J.G. Surface processing to improve the fatigue resistance of advanced bar steels for automotive applications. *Mater. Res.* **2005**, *8*, 453–459. https://doi.org/10.1590/S1516-14392005000400017.
2. Collins, J.A.; Busby, H.R.; Staab, G.H. *Mechanical Design of Machine Elements and Machines: A Failure Prevention Perspective*, 2nd ed.; John Wiley and Sons: Hoboken, NJ, USA, 2010.
3. Suresh, S. *Fatigue of Materials*, 2nd ed.; Cambridge University Press: Cambridge, MA, USA, 2004.
4. Juijerm, P.; Altenberger, I. Fatigue Performance Enhancement of Steels using Mechanical Surface Treatments. *J. Met. Mater. Miner.* **2007**, *17*, 59–65. Available online: https://www.researchgate.net/publication/237276226 (accessed on 15 January 2020).
5. Kumar, D.; Idapalapati, S.; Wang, W.; Narasimalu, S. Effect of surface mechanical treatments on the microstructure property performance of engineering alloys. *Materials* **2019**, *12*, 2503. https://doi.org/10.3390/ma12162503.
6. Zinn, W.; Scholtes, B. Mechanical surface treatments of lightweight materials: Effects on fatigue strength and near surface microstructures. *J. Mater. Eng. Perform.* **1999**, *8*, 145–151. https://doi.org/10.1361/105994999770346972.

7. Altenberger, I.; Scholtes, B. Recent developments in mechanical surface optimization. *Mater. Sci. Forum* **2000**, *347*, 382–398. https://doi.org/10.4028/www.scientific.net/msf.347-349.382.
8. Tolga Bozdana, A. On the mechanical surface enhancement techniques in aerospace industry—A review of technology. *Aircr. Eng. Aerosp. Technol.* **2005**, *77*, 279–292. https://doi.org/10.1108/00022660510606349.
9. Altenberger, I. Alternative mechanical surface treatments: Microstructures, residual stresses and fatigue behavior. In *Shot Peening*; Wagner, L., Ed.; Wiley-VCH Verlag GmbH and Co.: Hoboken, NJ, USA, 2006; pp. 419–434. https://doi.org/10.1002/3527606580.ch54.
10. Klumpp, A.; Hoffmeister, J.; Schulze, V. Mechanical Surface Treatments. In Proceedings of the 12th International Conference on Shot Peening, Goslar, Germany, 15–18 September 2014; pp. 12–24. Available online: https://www.shotpeener.com/library/pdf/2014044.pdf (accessed on 20 March 2020).
11. Schulze, V.; Bleicher, F.; Groche, P.; Guo, Y.B.; Pyun, Y.S. Surface modification by machine hammer peening and burnishing. *CIRP Ann.* **2016**, *65*, 809–832. https://doi.org/10.1016/j.cirp.2016.05.005.
12. Altenberger, I. Deep rolling: The past, the present and the future. In Proceedings of the 9th International Conference on Shot Peening, Paris, France, 6–9 September 2005; pp. 144–155. Available online: https://www.shotpeener.com/library/pdf/2005065.pdf (accessed on 6 April 2020).
13. Delgado, P.; Cuesta, I.I.; Alegre, J.M.; Díaz, A. State of the art of deep rolling. *Precis. Eng.* **2016**, *46*, 1–10. https://doi.org/10.1016/j.precisioneng.2016.05.001.
14. Borchers, F. Comparison of different manufacturing processes of AISI 4140 steel with regard to surface modification and its influencing depth. *Metals* **2020**, *10*, 895. https://doi.org/10.3390/met10070895.
15. Schulze, V. *Modern Mechanical Surface Treatment: States, Stability, Effects*; Wiley-VCH Verlag Gmbh and Co.: Hoboken, NJ, USA, 2005. https://doi.org/10.1002/3527607811.
16. Sonntag, R.; Reinders, J.; Gibmeier, J.; Kretzer, J.P. Fatigue performance of medical Ti6Al4V alloy after mechanical surface treatments. *PLoS ONE* **2015**, *10*, e0121963. https://doi.org/10.1371/journal.pone.0121963.
17. Abrão, A.M.; Denkena, B.; Köhler, J.; Breidenstein, B.; Mörke, T.; Rodrigues, P.C.M. The influence of heat treatment and deep rolling on the mechanical properties and integrity of AISI 1060 steel. *J. Mater. Process. Technol.* **2014**, *214*, 3020–3030. https://doi.org/10.1016/j.jmatprotec.2014.07.013.
18. Oevermann, T.; Saalfeld, S.; Niendorf, T.; Scholtes, B. Fatigue properties of steels SAE 1045 and SAE 4140 upon integrated inductive heat treatment and deep rolling at elevated temperature. In Proceedings of the 13th International Conference on Shot Peening, Montreal, QC, Canada, 18–21 September 2017; pp. 446–451. Available online: https://www.shotpeener.com/library/pdf/2017111.pdf (accessed on 4 March 2020).
19. Juijerm, P.; Altenberger, I.; Scholtes, B. Fatigue and residual stress relaxation of deep rolled differently aged aluminium alloy AA6110. *Mater. Sci. Eng. A* **2006**, *426*, 4–10. https://doi.org/10.1016/j.msea.2005.11.064.
20. Altenberger, I.; Nikitin, I.; Scholtes, B. Static and dynamic strain ageing of deep-rolled plain carbon steel SAE 1045 for optimized fatigue strength. In Proceedings of the 9th International Conference on Shot Peening, Marne La Vallee, France, 6–8 September 2005; pp. 253–260. Available online: http://www.shotpeener.com/library/pdf/2005094.pdf (accessed on 6 April 2020).
21. Wong, C.C.; Hartawan, A.; Teo, W.K. Deep cold rolling of features on aero-engine components. *Procedia CIRP* **2014**, *13*, 350–354. https://doi.org/10.1016/j.procir.2014.04.059.
22. Klocke, F.; Shirobokov, A.; Trauth, D.; Mattfeld, P. Deep rolling of fine blanking punch edges: Numerical and experimental investigation of a novel deep rolling tool for filleting of cylindrical punches. *Int. J. Mater. Form.* **2016**, *9*, 489–498. https://doi.org/10.1007/s12289-015-1235-x.
23. Nataliya, L.; Dirk, B. Finite element modelling and investigation of the process parameters in deep rolling of AISI 4140 steel. *J. Mater. Sci. Eng. B* **2015**, *5*, 277–287. https://doi.org/10.17265/2161-6221/2015.7-8.004.
24. Roller Burnishing, Deep Rolling, Cylinder Tube Processing. ECOROLL AG. Available online: https://www.ecoroll.de/en/ecoroll.html (accessed on 19 May 2021).
25. Crankshaft Manufacturer and Remanufacturer. Ellwood Crankshaft Group. Available online: www.ellwoodcrankshaftgroup.com (accessed on 19 May 2021).
26. Eigenmann, B.; Holzwarth, U.; Kachler, W.; Goske, J.; Wilcke, G.; Schuh, A. Deep rolling of titanium rods for application in total hip arthroplasty. In Proceedings of the 9th International Conference on Shot Peening, Paris, France, 6–9 September 2005; pp. 314–318. Available online: https://www.shotpeener.com/library/pdf/2005103.pdf (accessed on 4 March 2020).
27. Schuh, A. Deep rolling of titanium rods for application in modular total hip arthroplasty. *J. Biomed. Mater. Res. Part B Appl. Biomater.* **2007**, *81B*, 330–335. https://doi.org/10.1002/jbm.b.30669.
28. Bauccio, A. (Ed.) *ASM Metals Reference Book*, 3rd ed.; ASM International: Materials Park, OH, USA, 1993. https://doi.org/10.1016/0001-6160(56)90155-9.
29. Chemical Composition EN8 Steel and Equivalents. Shyam Metals. Available online: http://shyammetal.com (accessed on 9 January 2020).
30. Kloos, K.H.; Fuchsbauer, B.; Adelmann, J. Fatigue properties of specimens similar to components deep rolled under optimized conditions. *Int. J. Fatigue* **1987**, *9*, 35–42. https://doi.org/10.1016/0142-1123(87)90087-9.
31. Meyer, D.; Kämmler, J. Sustainable approach of heat treatment free surface hardening by deep rolling. *Int. J. Sustain. Manuf.* **2018**, *4*, 64–78. https://doi.org/10.1504/IJSM.2018.099580.

32. Scheil, J.; Müller, C.; Steitz, M.; Groche, P. Influence of process parameters on surface hardening in hammer peening and deep rolling. *Key Eng. Mater.* **2013**, *554–557*, 1819–1827. https://doi.org/10.4028/www.scientific.net/KEM.554-557.1819.
33. Wang, Z.M.; Jia, Y.F.; Zhang, X.C.; Fu, Y.; Zhang, C.C.; Tu, S.T. Effects of different mechanical surface enhancement techniques on surface integrity and fatigue properties of Ti-6Al-4V: A review. *Crit. Rev. Solid State Mater. Sci.* **2019**, *44*, 445–469. https://doi.org/10.1080/10408436.2018.1492368.
34. Juijerm, P.; Altenberger, I. Fatigue performance of high temperature deep rolled metallic materials. *J. Met. Mater. Miner.* **2007**, *17*, 37–41. Available online: https://pdfs.semanticscholar.org/792f /e829a700e17bd1fe011358a3428468ee15dd.pdf (accessed on 1 June 2020).
35. Altenberger, I.; Nikitin, I.; Juijerm, P.; Scholtes, B. Residual stress stability in high temperature fatigued mechanically surface treated metallic materials. *Mater. Sci. Forum* **2006**, *524–525*, 57–62. https://doi.org/10.4028/www.scientific.net/msf.524-525.57.
36. Abrão, A.M.; Denkena, B.; Köhler, J.; Breidenstein, B.; Mörke, T. The inducement of residual stress through deep rolling of AISI 1060 steel and its subsequent relaxation under cyclic loading. *Int. J. Adv. Manuf. Technol.* **2015**, *79*, 1939–1947. https://doi.org/10.1007/s00170-015-6946-0.
37. Dos Santos, F.F.; Silva, S.C.; Abrão, A.M.; Denkena, B.; Breidenstein, B.; Meyer, K. Influence of deep rolling on the surface integrity of AISI 1020 steel. *Rev. Mater.* **2020**, *25*, 1–13. https://doi.org/10.1590/S1517-707620200002.1051.
38. Dos, S.F.F.; Silva, S.D.C.; Abrão, A.M.; Denkena, B.; Breidenstein, B.; Meyer, K. Influence of the carbon content on the surface integrity of deep rolled steels. *J. Tribol.* **2021**, *143*, 081702. https://doi.org/10.1115/1.4049109.
39. Nikitin, I.; Altenberger, I.; Scholtes, B. Effect of deep rolling at elevated and low temperatures on the isothermal fatigue behavior of AISI 304. In Proceedings of the 9th International Conference on Shot Peening, Paris, France, 6–9 September 2005; pp. 185–190. Available online: http://www.shotpeener.com/library/pdf/2005070.pdf (accessed on 6 April 2020).
40. Nikitin, I.; Besel, M. Residual stress relaxation of deep rolled austenitic steel. *Scr. Mater.* **2008**, *58*, 239–242. https://doi.org/10.1016/j.scriptamat.2007.09.045.
41. Altenberger, I.; Scholtes, B.; Martin, U.; Oettel, H. Cyclic deformation and near surface microstructures of shot peened or deep rolled austenitic stainless steel AISI 304. *Mater. Sci. Eng. A* **1999**, *264*, 1–16. https://doi.org/10.1016/S0921-5093(98)01121-6.
42. Muñoz-Cubillos, J.; Coronado, J.J.; Rodríguez, S.A. Deep rolling effect on fatigue behavior of austenitic stainless steels. *Int. J. Fatigue* **2017**, *95*, 120–131. https://doi.org/10.1016/j.ijfatigue.2016.10.008.
43. Tadi, A.J. Formation of surface nano/ultrafine structure using deep rolling process on the AISI 316L stainless steel. *Mater. Sci. Eng. Int. J.* **2017**, *1*, 88–93. https://doi.org/10.15406/mseij.2017.01.00015.
44. Prabhu, P.R.; Sharma, S.S.; Kulkarni, S.M.; Gowrishankar, M.C. Turn-assisted deep cold rolling: An innovative manufacturing method for the improvement of fatigue life. *Int. J. Appl. Eng. Res.* **2015**, *10*, 64–68.
45. Prabhu, P.R.; Kulkarni, S.M.; Sharma, S.S. Multi response optimization of the turn-assisted deep cold rolling process parameters for enhanced surface characteristics and residual stress of AISI 4140 steel shafts. *J. Mater. Res. Technol.* **2020**, *9*, 11402–11423. https://doi.org/10.1016/j.jmrt.2020.08.025.
46. Prabhu, P.R.; Prabhu, D.; Sharma, S.; Kulkarni, S.M. Surface properties and corrosion behavior of turn assisted deep cold rolled AISI 4140 steel. *J. Mater. Eng. Perform.* **2020**, *29*, 5871–5885. https://doi.org/10.1007/s11665-020-05051-x.
47. Lyubenova, N. Impact of the process parameters, the measurement conditions and the pre-machining on the residual stress state of deep rolled specimens. *J. Manuf. Mater. Process.* **2019**, *3*, 56. https://doi.org/10.3390/jmmp3030056.
48. Martins, A.M.; Rodrigues, P.C.; Abrão, A.M. Influence of machining parameters and deep rolling on the fatigue life of AISI 4140 steel. *Int. J. Adv. Manuf. Technol.* **2022**, *121*, 6153–6167. https://doi.org/10.1007/s00170-022-09703-1.
49. Martins, A.M.; Oliveira, D.A.D.; de Castro Magalhães, F.; Abrão, A.M. Relationship between surface characteristics and the fatigue life of deep rolled AISI 4140 steel. *Int. J. Adv. Manuf. Technol.* **2023**, *129*, 1127–1143. https://doi.org/10.1007/s00170-023-12332-x.
50. Meyer, D.; Kämmler, J. Surface integrity of AISI 4140 after deep rolling with varied external and internal loads. *Procedia CIRP* **2016**, *45*, 363–366. https://doi.org/10.1016/j.procir.2016.02.356.
51. Kämmler, J.; Wielki, N.; Meyer, D. Surface integrity after internal load oriented multistage contact deep rolling. *Procedia CIRP* **2018**, *71*, 490–495. https://doi.org/10.1016/j.procir.2018.05.026.
52. Luo, X. Effect of deep surface rolling on microstructure and properties of AZ91 magnesium alloy. *Trans. Nonferrous Met. Soc. China (Engl. Ed.)* **2019**, *29*, 1424–1429. https://doi.org/10.1016/S1003-6326(19)65049-1.
53. Salahshoor, M.; Guo, Y.B. Process mechanics in deep rolling of magnesium-calcium (Mgca) biomaterial. In Proceeding of the 2011 ASME International Manufacturing Science and Engineering Conference MSEC2011, Corvallis, OR, USA, 13–17 June 2017; pp. 1–9. Available online: http://proceedings.asmedigitalcollection.asme.org/pdfaccess.ashx?url=/data/conferences/msec2011/69845/ (accessed on 12 March 2020).
54. Noster, U.; Altenberger, I.; Scholtes, B. Combined mechanical and thermal surface treatment of magnesium wrought alloy AZ31. *Comput. Exp. Methods* **2001**, *6*, 3–12. https://doi.org/10.2495/SURF010001.
55. Xin, C.; Sun, Q.; Xiao, L.; Sun, J. Biaxial fatigue property enhancement of gradient ultra-fine-grained Zircaloy-4 prepared by surface mechanical rolling treatment. *J. Mater. Sci.* **2018**, *53*, 12492–12503. https://doi.org/10.1007/s10853-018-2391-4.
56. Juijerm, P.; Altenberger, I. Effects of deep rolling and its modification on fatigue performance of aluminium alloy AA6110. In *Aluminium Alloys: New Trends in Fabrication and Applications*; Ahmad, Z., Ed.; Intech Open: London, UK, 2012; Chapter 5, pp. 123–136. https://doi.org/10.5772/50651.

57. Juijerm, P.; Noster, U.; Altenberger, I.; Scholtes, B. Fatigue of deep rolled AlMg4.5Mn (AA5083) in the temperature range 20-300 °C. *Mater. Sci. Eng. A* **2004**, *379*, 286–292. https://doi.org/10.1016/j.msea.2004.02.022.
58. Juijerm, P.; Altenberger, I. Effective boundary of deep-rolling treatment and its correlation with residual stress stability of Al-Mg-Mn and Al-Mg-Si-Cu alloys. *Scr. Mater.* **2007**, *56*, 745–748. https://doi.org/10.1016/j.scriptamat.2007.01.021.
59. Mombeini, D.; Atrian, A. Experimental and numerical investigation of the effects of deep cold rolling on the bending fatigue tolerance of C38500 brass alloy. *Int. J. Adv. Manuf. Technol.* **2018**, *97*, 3039–3053. https://doi.org/10.1007/s00170-018-2165-9.
60. Majzoobi, G.H.; Jouneghani, F.Z.; Khademi, E. Experimental and numerical studies on the effect of deep rolling on bending fretting fatigue resistance of Al7075. *Int. J. Adv. Manuf. Technol.* **2016**, *82*, 2137–2148. https://doi.org/10.1007/s00170-015-7542-z.
61. Zhou, Y.; Chu, X.; Zang, S.; Sun, J.; Yang, L.; Gao, J. Effect of surface integrity on fatigue life of 7075-T6 aluminum alloy by combination of fine turning with hydrostatic deep rolling. *Arch. Civ. Mech. Eng.* **2022**, *23*, 41. https://doi.org/10.1007/s43452-022-00580-9.
62. Lehmann, J.; Keller, S.; Esterl, F.; Kashaev, N.; Klusemann, B.; Ben Khalifa, N. Deep Rolling for Tailoring Residual Stresses of AA2024 Sheet Metals. In *Proceedings of the 14th International Conference on the Technology of Plasticity—Current Trends in the Technology of Plasticity. ICTP 2023. Lecture Notes in Mechanical Engineering*; Mocellin, K., Bouchard, P.O., Bigot, R., Balan, T., Eds.; Springer: Cham, Switzerland, 2024; pp. 352–362. https://doi.org/10.1007/978-3-031-41341-4_37.
63. Kloos, K.H.; Adelmann, J. Effect of deep rolling on fatigue properties of cast irons. *J. Mech. Behav. Mater.* **2011**, *2*, 75–86. https://doi.org/10.1515/jmbm.1989.2.1-2.75.
64. Nagarajan, B.; Kumar, D.; Fan, Z.; Castagne, S. Effect of deep cold rolling on mechanical properties and microstructure of nickel-based superalloys. *Mater. Sci. Eng. A* **2018**, *728*, 196–207. https://doi.org/10.1016/j.msea.2018.05.005.
65. Kumar, D.; Idapalapati, S.; Wang, W.; Bhowmik, A. Microstructural characteristics and strengthening mechanisms in a polycrystalline Ni-based superalloy under deep cold rolling. *Mater. Sci. Eng. A* **2019**, *753*, 285–299. https://doi.org/10.1016/j.msea.2019.03.005.
66. Lindemann, J.; Grossmann, K.; Raczek, T.; Wagner, L. Influence of shot peening and deep rolling on high temperature fatigue of the Ni-superalloy udimet 720 LI. In *Shot Peening*; Wagner, L., Ed.; Wiley Online Library: Hoboken, NJ, USA, 2006; pp. 454–460. https://doi.org/10.1002/3527606580.ch58.
67. Lim, A.; Castagne, S.; Wong, C.C. Effect of deep cold rolling on residual stress distributions between the treated and untreated regions on Ti-6Al-4V alloy. *J. Manuf. Sci. Eng.* **2016**, *138*, 111005. https://doi.org/10.1115/1.4033524.
68. Nalla, R.K.; Altenberger, I.; Noster, U.; Liu, G.Y.; Scholtes, B.; Ritchie, R.O. On the influence of mechanical surface treatments-deep rolling and laser shock peening-on the fatigue behavior of Ti-6Al-4V at ambient and elevated temperatures. *Mater. Sci. Eng. A* **2003**, *355*, 216–230. https://doi.org/10.1016/S0921-5093(03)00069-8.
69. Han, K.; Zhang, D.; Yao, C.; Tan, L.; Zhou, Z.; Zhao, Y. Investigation of residual stress distribution induced during deep rolling of Ti-6Al-4V alloy. *Proc. Inst. Mech. Eng. Part B J. Eng. Manuf.* **2021**, *235*, 186–197. https://doi.org/10.1177/0954405420947960.
70. Sattari, S.; Atrian, A. Effects of the deep rolling process on the surface roughness and properties of an Al–3vol%SiC nanoparticle nanocomposite fabricated by mechanical milling and hot extrusion. *Int. J. Miner. Metall. Mater.* **2017**, *24*, 814–825. https://doi.org/10.1007/s12613-017-1465-7.
71. Sattari, S.; Atrian, A. Investigation of deep rolling effects on the fatigue life of Al-SiC nanocomposite. *Mater. Res. Express* **2018**, *5*, 015052. https://doi.org/10.1088/2053-1591/aaa566.
72. Wagner, L. Mechanical surface treatments on titanium, aluminium and magnesium alloys. *Mater. Sci. Eng. A* **1999**, *263*, 210–216. https://doi.org/10.1016/s0921-5093(98)01168-x.
73. Saalfeld, S.; Wegener, T.; Scholtes, B.; Niendorf, T.; Thermal stability of residual stresses in differently deep rolled surface layers of steel SAE 1045. *J. Mater. Eng. Perform.* **2021**, *30*, 6160–6166. https://doi.org/10.1007/s11665-021-05798-x.
74. Oevermann, T.; Wegener, T.; Niendorf, T. On the evolution of residual stresses, microstructure and cyclic performance of high manganese austenitic TWIP steel after deep rolling. *Metals* **2019**, *9*, 825. https://doi.org/10.3390/met9080825.
75. Cherif, A.; Hochbein, H.; Zinn, W.; Scholtes, B. Increase of fatigue strength and lifetime by deep rolling at elevated temperature of notched specimens made of steel SAE 4140. *HTM J. Heat Treat. Mater.* **2011**, *66*, 342–348. https://doi.org/10.3139/105.110120.
76. Primee, S.Y.; Juijerm, P. Modified mechanical surface treatment for optimized fatigue performance of martensitic stainless steel AISI 420. *Met. Mater. Int.* **2019**, *27*, 946–952. https://doi.org/10.1007/s12540-019-00517-7.
77. Meyer, D. Cryogenic deep rolling: An energy-based approach for enhanced cold surface hardening. *CIRP Ann.* **2012**, *61*, 543–546. https://doi.org/10.1016/j.cirp.2012.03.102.
78. Usami, H.; Sato, S.; Saito, M.; Ando, M. Combined effects of micro shot peening and deep rolling on the fatigue. In Proceedings of the 13th International Conference on shot Peening (ICSP-13), Montreal, QC, Canada, 18–21 September 2017; pp. 478–482. Available online: https://www.shotpeener.com/library/pdf/2017116.pdf (accessed on 4 March 2020).
79. Gopinath, A.; Lim, A.; Nagarajan, B.; Wong, C.C.; Maiti, R.; Castagne, S. Introduction of enhanced compressive residual stress profiles in aerospace components using combined mechanical surface treatments. *IOP Conf. Ser. Mater. Sci. Eng.* **2016**, *157*, 012013. https://doi.org/10.1088/1757-899X/157/1/012013.
80. Gryadunov, I.M.; Radchenko, S.Y.; Dorokhov, D.O.; Morrev, P.G. Deep hardening of inner cylindrical surface by periodic deep rolling—Burnishing process. *Mod. Appl. Sci.* **2015**, *9*, 251–258. https://doi.org/10.5539/mas.v9n9p251.
81. Zheng, J.; Hou, Y.; Ming, P. Basic experiment of ultrasonic deep rolling with longitudinal-torsional vibration. *Key Eng. Mater.* **2016**, *667*, 29–34. https://doi.org/10.4028/www.scientific.net/KEM.667.29.

82. Bozdana, A.T.; Gindy, N.N.Z.; Li, H. Deep cold rolling with ultrasonic vibrations—A new mechanical surface enhancement technique. *Int. J. Mach. Tools Manuf.* **2005**, *45*, 713–718. https://doi.org/10.1016/j.ijmachtools.2004.09.017.
83. Zhang, M.; Liu, Z.; Deng, J.; Yang, M.; Dai, Q.; Zhang, T. Optimum design of compressive residual stress field caused by ultrasonic surface rolling with a mathematical model. *Appl. Math. Model.* **2019**, *76*, 800–831. https://doi.org/10.1016/j.apm.2019.07.009.
84. Ren, S. Enhanced surface mechanical properties of Cr12MoV using ultrasonic surface rolling process and deep cryogenic treatment. *Solid State Phenom.* **2018**, *279*, 143–147. https://doi.org/10.4028/www.scientific.net/SSP.279.143.
85. Kuhlemann, P.; Denkena, B.; Krödel, A.; Beblein, S. Influence of thermal effects in turn-rolling. *CIRP J. Manuf. Sci. Technol.* **2020**, *31*, 294–304. https://doi.org/10.1016/j.cirpj.2020.06.003.
86. Martins, A.M.; Leal, C.A.; Campidelli, A.F.; Abrao, A.M.; Rodrigues, P.C.; Magalhães, F.C.; Denkena, B.; Meyer, K. Assessment of the temperature distribution in deep rolling of hardened AISI 4140 steel. *J. Manuf. Process.* **2022**, *73*, 686–694. https://doi.org/10.1016/j.jmapro.2021.11.052.
87. Breidenstein, B.; Wichmann, M.; Voelker, H. Marker-free identification of turned, ground and deep rolled workpieces using wavelet transformation. *Procedia CIRP* **2023**, *118*, 1120–1125. https://doi.org/10.1016/j.procir.2023.06.192.
88. Strodick, S.; Vogel, F.; Tilger, M.; Denstorf, M.; Kipp, M.; Baak, N.; Kukui, D.; Biermann, D.; Barrientos, M.M.; Walther, F. Innovative X-ray diffraction and micromagnetic approaches for reliable residual stress assessment in deep rolled and microfinished AISI 4140 components. *J. Mater. Res. Technol.* **2022**, *20*, 2942–2959. https://doi.org/10.1016/j.jmrt.2022.07.168.
89. Maiß, O.; Röttger, K. Monitoring the Surface Quality for Various Deep Rolling Processes–Limits and Experimental Results. *Procedia CIRP* **2022**, *108*, 857–862. https://doi.org/10.1016/j.procir.2022.05.199.
90. Lyubenova, N.; Jacquemin, M.; Bähre, D.; Influence of the pre-stressing on the residual stresses induced by deep rolling. *Mater. Res. Proc.* **2016**, *2*, 253–258. https://doi.org/10.21741/9781945291173-43.
91. Mueller, E. A systematic investigation of the induced residual stresses by deep rolling in dependence of the prestress at spring steel. In Proceedings of the 13th International Conference on shot Peening (ICSP-13), Montreal, QC, Canada, 18–21 September 2017; pp. 401–406. Available online: https://www.shotpeener.com/library/pdf/2017103.pdf (accessed on 6 March 2020).
92. Jia, Y.F. Enhanced surface strengthening of titanium treated by combined surface deep-rolling and oxygen boost diffusion technique. *Corros. Sci.* **2019**, *157*, 256–267. https://doi.org/10.1016/j.corsci.2019.05.020.
93. Yutanorm, W.; Juijerm, P. Diffusion enhancement of low-temperature pack aluminizing on austenitic stainless steel AISI 304 by deep rolling process. *Kov. Mater.* **2016**, *54*, 227–232. https://doi.org/10.4149/km_2016_3_227.
94. Axinte, D.A.; Gindy, N. Turning assisted with deep cold rolling—A cost efficient hybrid process for workpiece surface quality enhancement. *Proc. Inst. Mech. Eng. Part B J. Eng. Manuf.* **2004**, *218*, 807–811. https://doi.org/10.1177/095440540421800713.
95. Denkena, B.; Poll, G.; Maiß, O.; Neubauer, T. Affecting the life time of roller bearings by an optimal surface integrity design after hard turning and deep rolling. *Adv. Mater. Res.* **2014**, *966–967*, 425–434. https://doi.org/10.4028/www.scientific.net/AMR.966-967.425.
96. Maiß, O.; Denkena, B.; Grove, T. Hybrid machining of roller bearing inner rings by hard turning and deep rolling. *J. Mater. Process. Technol.* **2016**, *230*, 211–216. https://doi.org/10.1016/j.jmatprotec.2015.11.029.
97. Guan, R.G.; Wang, X.; Zhao, Z.Y.; Wang, W.W.; Cao, F.R.; Liu, C.M. Microstructure and properties of A2017 alloy strips processed by a novel process by combining semisolid rolling, deep rolling, and heat treatment. *Int. J. Miner. Metall. Mater.* **2013**, *20*, 770–778. https://doi.org/10.1007/s12613-013-0795-3.
98. Zhao, Z.Y. Effects of dynamic recrystallisation during deep rolling of semisolid slab and heat treatment on microstructure and properties of AZ31 alloy. *Mater. Sci. Technol.* **2014**, *30*, 309–315. https://doi.org/10.1179/1743284713Y.0000000343.
99. Meyer, D.; Wielki, N. Internal reinforced domains by intermediate deep rolling in additive manufacturing. *CIRP Annals* **2019**, *68*, 579–582. https://doi.org/10.1016/j.cirp.2019.04.012.
100. Hönnige, J.R. Residual stress and texture control in Ti-6Al-4V wire + arc additively manufactured intersections by stress relief and rolling. *Mater. Des.* **2018**, *150*, 193–205. https://doi.org/10.1016/j.matdes.2018.03.065.
101. Uhlmann, L.; Weiser, I.F.; Herrig, T.; Bergs, T. Deep Rolling of Bores Using Centrifugal Force. *Eng. Proc.* **2022**, *26*, 20. https://doi.org/10.3390/engproc2022026020.
102. Wielki, N.; Heinz, N.; Meyer, D. Characterizing the local material properties of different Fe–C–Cr-steels by using deep rolled single tracks. *Materials* **2020**, *13*, 4987. https://doi.org/10.3390/ma13214987.
103. Yentzer, T.; Stillman, B.; Fisher, M.; Pardue, B.; Krafsur, D.; Khaled, T. Fatigue life and residual stresses in cold rolled propeller blades. In Proceedings of the Conference on Aging Aircrafts, Albuquerque, Mexico, 1999; pp. 1–24. Available online: https://citeseerx.ist.psu.edu/document?repid=rep1&type=pdf&doi=379f667d02f0ca5e5477c2db471d89c7f4921a2e (accessed on 12 August 2019).
104. Schieber, C.; Hettig, M.; Zaeh, M.F.; Heinzel, C. Combination of Thermal and Mechanical Strategies to Compensate for Distortion Effects during Profile Grinding. *Machines* **2022**, *10*, 1240. https://doi.org/10.3390/machines10121240.
105. Klocke, F.; Mader, S.; Fundamentals of the deep rolling of compressor blades for turbo aircraft engines. *Steel Res. Int.* **2005**, *76*, 229–235. https://doi.org/10.1002/srin.200506001.
106. Zhuang, W.; Wicks, B. Mechanical surface treatment technologies for gas turbine engine components. *J. Eng. Gas Turbines Power* **2003**, *125*, 1021–1025. https://doi.org/10.1115/1.1610011.
107. Fu, H.; Liu, Y.; Xu, Q.; Yan, X.; Yang, G.; Chen, H. Effect of deep rolling parameters on surface integrity of LZ50 axles. *Int. J. Mod. Phys. B* **2019**, *33*, 1950298. https://doi.org/10.1142/S0217979219502989.

108. Regazzi, D.; Beretta, S.; Carboni, M. An investigation about the influence of deep rolling on fatigue crack growth in railway axles made of a medium strength steel. *Eng. Fract. Mech.* **2014**, *131*, 587–601. https://doi.org/10.1016/j.engfracmech.2014.09.016.
109. Pertoll, T.; Buzzi, C.; Dutzler, A.; Leitner, M.; Seisenbacher, B.; Winter, G.; Boronkai, L. Experimental and numerical investigation of the deep rolling process focusing on 34CrNiMo6 railway axles. *Int. J. Mater. Form.* **2023**, *16*, 51. https://doi.org/10.1007/s12289-023-01775-y.
110. Udalov, A.A.; Parshin, S.V.; Udalov, A.V.; Vasilevykh, S.L. Power parameters of the process of hardening of cylindrical parts by a toroidal roller by the method of surface plastic deformation. *J. Phys. Conf. Ser.* **2019**, *1210*, 012150. https://doi.org/10.1088/1742-6596/1210/1/012150.
111. Qiao, Y.; Chen, H.; Qi, K.; Guo, P. Research on mechanical properties of 210cr12 shaft surface processed with rolling. *Coatings* **2020**, *10*, 611. https://doi.org/10.3390/coatings10070611.
112. Galzy, F.; Michaud, H.; Sprauel, J.M. Approach of residual stress generated by deep rolling application to the reinforcement of the fatigue resistance of crankshafts. *Mater. Sci. Forum* **2005**, *490–491*, 384–389. https://doi.org/10.4028/www.scientific.net/msf.490-491.384.
113. Michaud, H.; Sprauel, J.M.; Galzy, F. The residual stresses generated by deep rolling and their stability in fatigue and application to deep rolled crankshafts. *Mater. Sci. Forum* **2006**, *524–525*, 45–50. https://doi.org/10.4028/www.scientific.net/msf.524-525.45.
114. Cevik, M.C.; Hochbein, H.; Rebbert, M. Potentials of crankshaft fillet rolling process. *SAE Int. J. Engines* **2012**, *5*, 622–632. https://doi.org/10.4271/2012.01.0755.
115. Bertini, L.; Santus, C.; Merlo, A.; Bandini, M. A fretting fatigue setup for testing shrink-fit connections and experimental evidence of the strength enhancement induced by deep rolling. *Proc. Inst. Mech. Eng. Part C J. Mech. Eng. Sci.* **2016**, *230*, 1432–1439. https://doi.org/10.1177/0954406215612817.
116. Cheng, M.; Zhang, D.; Chen, H.; Qin, W. Development of ultrasonic thread root rolling technology for prolonging the fatigue performance of high strength thread. *J. Mater. Process. Technol.* **2014**, *214*, 2395–2401. https://doi.org/10.1016/j.jmatprotec.2014.05.019.
117. Wang, X.; Xiong, X.; Huang, K.; Ying, S.; Tang, M.; Qu, X.; Ji, W.; Qian, C.; Cai, Z. Effects of Deep Rolling on the Microstructure Modification and Fatigue Life of 35Cr2Ni4MoA Bolt Threads. *Metals* **2022**, *12*, 1224. https://doi.org/10.3390/met12071224.
118. Reggiani, B.; Olmi, G. Experimental investigation on the effect of shot peening and deep rolling on the fatigue response of high strength fasteners. *Metals* **2019**, *9*, 1093. https://doi.org/10.3390/met9101093.
119. Perenda, J.; Trajkovski, J.; Žerovnik, A.; Prebil, I. Modeling and experimental validation of the surface residual stresses induced by deep rolling and presetting of a torsion bar. *Int. J. Mater. Form.* **2016**, *9*, 435–448. https://doi.org/10.1007/s12289-015-1230-2.
120. Močilnik, V.; Gubeljak, N.; Predan, J. Effect of residual stresses on the fatigue behaviour of torsion bars. *Metals* **2020**, *10*, 1056. https://doi.org/10.3390/met10081056.
121. Maiß, O.; Röttger, K.; Meyer, K. Increase the Ressource Efficiency by Evaluation of the Effects of Deep Rolling within the Design and Manufacturing Phase. *In Future Automotive Production Conference 2022, Zukunftstechnologien für den Multifunktionalen Leichtbau*; Dröder, K., Vietor, T., Eds.; Springer: Wiesbaden, Germany, 2023; pp. 86–96. https://doi.org/10.1007/978-3-658-39928-3_7.
122. Baisukhan, A.; Nakkiew, W. Influence of deep rolling process parameters on surface residual stress of aa7075-t651 aluminum alloy friction stir welded joint. *Mater. Sci. Forum* **2018**, *939*, 23–30. https://doi.org/10.4028/www.scientific.net/MSF.939.23.
123. Baisukhan, A.; Nakkiew, W. Effects of deep rolling on surface residual stress and Microhardness of JIS SS400 MIG welding. *Mater. Sci. Forum* **2018**, *939*, 31–37. https://doi.org/10.4028/www.scientific.net/MSF.939.31.
124. Heikebrügge, S.; Breidenstein, B.; Bergmann, B.; Dänekas, C.; Schaumann, P. Experimental and Numerical Investigations of the Deep Rolling Process to Analyze the Local Deformation Behavior of Welded Joints. *J. Manuf. Mater. Process.* **2022**, *6*, 50. https://doi.org/10.3390/jmmp6030050.
125. Dänekas, C.; Heikebrügge, S.; Schubnell, J.; Schaumann, P.; Breidenstein, B.; Bergmann, B. Influence of deep rolling on surface layer condition and fatigue life of steel welded joints. *Int. J. Fatigue* **2022**, *162*, 106994. https://doi.org/10.1016/j.ijfatigue.2022.106994.
126. Schubnell, J.; Dahmen, M.; Luke, M. Strength improvement of laser beam welded joints in cold worked high-manganese-steel by means of deep rolling. *Procedia CIRP* **2022**, *111*, 457–461. https://doi.org/10.1016/j.procir.2022.08.065.
127. Bhargava, V.; Hahn, G.T.; Rubin, C.A.; An elastic-plastic finite element model of rolling contact. Part 1: Analysis of single contacts. *J. Appl. Mech.* **1985**, *52*, 67–74.
128. Bhargava, V.; Hahn, G.T.; Rubin, C.A.; An elastic-plastic finite element model of rolling contact. Part 2: Analysis of repeated contacts. *J. Appl. Mech.* **1985**, *52*, 75–82.
129. Donzella, G.; Guagliano, M.; Vergani, L. Experimental investigations and numerical analyses on deep rolling residual stresses. *Trans. Eng. Sci.* **1993**, *2*, 589–598. https://doi.org/10.2495/SURF930021.
130. Guagliano, M.; Vergani, L.; Residual stresses induced by deep rolling in notched components. *J. Mech. Behav. Mater.* **1998**, *9*, 129–140. https://doi.org/10.1515/jmbm.1998.9.2.129.
131. Demurger, J.; Forestier, R.; Kieber, B.; Lasne, P. Deep rolling process simulation: Impact of kinematic hardening on residual stresses. In Proceedings of the 9th International Conference on Material Forming ESAFORM, Glasgow, UK, 26–28 April 2006; pp. 1–5. Available online: https://www.researchgate.net/profile/Demurger-Joelle/publication/283993247 (accessed on 3 March 2020).
132. Choi, K.S.; Pan, J. Simulations of stress distributions in crankshaft sections under fillet rolling and bending fatigue tests. *Int. J. Fatigue* **2009**, *31*, 544–557. https://doi.org/10.1016/j.ijfatigue.2008.03.035.

133. Majzoobi, G.H.; Azadikhah, K.; Nemati, J. The effects of deep rolling and shot peening on fretting fatigue resistance of Aluminum-7075-T6. *Mater. Sci. Eng. A* **2009**, *516*, 235–247. https://doi.org/10.1016/j.msea.2009.03.020.
134. Bäcker, V.; Klocke, F.; Wegner, H.; Timmer, A.; Grzhibovskis, R.; Rjasanow, S. Analysis of the deep rolling process on turbine blades using the FEM/BEM-coupling. *IOP Conf. Ser. Mater. Sci. Eng.* **2014**, *10*, 012134. https://doi.org/10.1088/1757-899X/10/1/012134.
135. Manouchehrifar, A.; Alasvand, K. Simulation and research on deep rolling process parameters. *Int. J. Adv. Des. Manuf. Technol.* **2012**, *5*, 31–37.
136. Nicoletto, G.; Saletti, A. Fatigue assessment of notched steel including residual stresses obtained by the rolling process. *SDHM Struct. Durab. Health Monit.* **2012**, *8*, 131–148. https://doi.org/10.3970/sdhm.2012.008.131.
137. Liou, J.J.; El-Wardany, T.I. Numerical investigation of lubricated deep rolling process in a complex roller path. *Adv. Mater. Res.* **2014**, *966–967*, 406–424. https://doi.org/10.4028/www.scientific.net/AMR.966-967.406.
138. Kumar, P.K.; Raviraj, A.; Prabhu, P.R.; Laxmikanth, K. Deep cold rolling simulation of AISI 4140 steel using ANSYS LSDYNA. In Proceedings of the 3rd World Conference on Applied Sciences, Engineering and Technology, San Francisco, CA, USA, 22–24 October 2014; pp. 27–29.
139. Lim, A.; Castagne, S.; Wong, C.C. Effect of friction coefficient on finite element modeling of the deep cold rolling process. In Proceedings of the 12th International Conference on Shot Peening, Goslar, Germany, 15–18 September 2014; Volume 12, pp. 376–380. Available online: https://www.shotpeener.com/library/pdf/2014106.pdf (accessed on 15 January 2020).
140. Hassani-Gangaraj, S.M.; Carboni, M.; Guagliano, M. Finite element approach toward an advanced understanding of deep rolling induced residual stresses, and an application to railway axles. *Mater. Des.* **2015**, *83*, 689–703. https://doi.org/10.1016/j.matdes.2015.06.026.
141. Lyubenova, N.; Bahre, D. The impact of the material modeling on the calculated residual stresses induced by deep rolling the impact of the material modeling on the calculated residual stresses induced by deep rolling. In Proceedings of the International Materials Research Meeting in the Greater Region: Current Trends in the Characterization of Materials and Surface Modification, Saarbruecken, Germany, 6–7 April 2017; pp. 65–66. Available online: https://www.researchgate.net/profile/Nataliya-Lyubenova/publication/317955696 (accessed on 4 March 2020).
142. Zaharevskis, V.; Kurushin, A.; Kovzels, O. Use of FEM numerical simulation approach for surface rolling process control. *Eng. Rural. Dev.* **2018**, *17*, 1378–1383. https://doi.org/10.22616/ERDev2018.17.N145.
143. Kinner-Becker, T.; Sölter, J.; Karpuschewski, B. A simulation-based analysis of internal material loads and material modifications in multi-step deep rolling. *Procedia CIRP* **2020**, *87*, 515–520. https://doi.org/10.1016/j.procir.2020.02.060.
144. Kinner-Becker, T.; Hettig, M.; Sölter, J.; Meyer, D. Analysis of internal material loads and Process Signature Components in deep rolling. *CIRP J. Manuf. Sci. Technol.* **2021**, *35*, 400–409. https://doi.org/10.1016/j.cirpj.2021.06.024.
145. Kinner-Becker, T.; Sölter, J. Influence of initial stress on the residual stress generated by deep rolling. *Procedia CIRP* **2023**, *117*, 128–132. https://doi.org/10.1016/j.procir.2023.03.023.
146. Bialowas, J.; Pletz, M.; Gapp, S.; Maierhofer, J. A method to reduce computation time in finite element simulations of deep rolling. *Procedia Struct. Integr.* **2023**, *46*, 49–55. https://doi.org/10.1016/j.prostr.2023.06.009.
147. Fonseca, L.G.A.; Faria, A.R.D. A deep rolling finite element analysis procedure for automotive crankshafts. *J. Strain Anal. Eng. Des.* **2018**, *53*, 178–188. https://doi.org/10.1177/0309324717751942.
148. Fonseca, L.G.A.; Faria, A.R.D. Crankshaft deep rolling analysis through energy balance simulation output. *J. Braz. Soc. Mech. Sci. Eng.* **2019**, *41*, 430. https://doi.org/10.1007/s40430-019-1932-3.
149. Pertoll, T.; Buzzi, C.; Leitner, M.; Boronkai, L. Numerical parameter sensitivity analysis of residual stresses induced by deep rolling for a 34CrNiMo6 steel railway axle. *Int. J. Adv. Manuf. Technol.* **2024**, *131*, 483–504. https://doi.org/10.1007/s00170-024-13039-3.
150. Morrev, P.G.; Gordon, V.A. Simulation of surface hardening in the deep rolling process by means of an axial symmetric nodal averaged finite element. *J. Phys. Conf. Ser.* **2018**, *973*, 012013. https://doi.org/10.1088/1742-6596/973/1/012013.
151. Heikebrügge, S.; Breidenstein, B.; Bergmann, B.; Dänekas, C.; Schaumann, P.; Schubnell, J. Identification of material properties for finite element simulation of the deep rolling process applied to welded joints. *Procedia CIRP* **2022**, *115*, 30–35. https://doi.org/10.1016/j.procir.2022.10.045.
152. Abrão, A.M.; Denkena, B.; Breidenstein, B.; Mörke, T. Surface and subsurface alterations induced by deep rolling of hardened AISI 1060 steel. *Prod. Eng.* **2014**, *8*, 551–558. https://doi.org/10.1007/s11740-014-0539-x.
153. Prabhu, P.R. Investigation on Effect of Process Parameters for Fatigue Life Improvement Using Turn Assisted Deep Cold Rolling Process. Ph.D. Thesis, Manipal University, Manipal, India, 2014.
154. Esme, U.; Sagbas, A.; Kahraman, F.; Kulekci, K. Use of artificial neural networks in ball burnishing process for the prediction of surface roughness of AA 7075 aluminum alloy. *Mater. Tehnol.* **2008**, *42*, 215–219.
155. Tang, S.H.; Hakim, N.; Khaksar, W.; Sulaiman, S.; Ariffin, M.K.A.; Samin, R. Artificial Neural Network (ANN) Approach for Predicting Friction Coefficient of Roller Burnishing AL6061. *Int. J. Mach. Learn. Comput.* **2012**, *2*, 825–830. Available online: https://www.ijmlc.org/papers/246-K30002.pdf (accessed on 3 March 2020).

156. Kluz, R.; Antosz, K.; Trzepieciński, T.; Bucior, M. Modelling the influence of slide burnishing parameters on the surface roughness of shafts made of 42CrMo4 heat-treatable steel. *Materials* **2021**, *14*, 1175. https://doi.org/10.3390/ma14051175.
157. Nguyen, T.T.; Nguyen, T.A.; Trinh, Q.H.; Le, X.B.; Pham, L.H.; Le, X.H. Artificial neural network-based optimization of operating parameters for minimum quantity lubrication-assisted burnishing process in terms of surface characteristics. *Neural Comput. Appl.* **2022**, *34*, 7005–7031. https://doi.org/10.1007/s00521-021-06834-6.